



TASMANIA
DEVELOPMENT
AND RESOURCES

Mineral Resources Tasmania

REPORT 1994/08

An interpretation of recent geophysical
surveys, northeastern Tasmania

by
R. G. Richardson
and
M. J. Roach

CONTENTS

Abstract	3
INTRODUCTION	4
REGIONAL OVERVIEW	4
Gravity field	4
Magnetic field	5
Synthesis of data sets	6
Quantitative interpretation	6
NETGOLD AREAS	7
Fingal area	7
Gravity field	7
Magnetic field	8
Radiometrics	9
Quantitative interpretation	9
Synthesis of data for the Fingal area	10
Northern coastal area	10
Gravity field	10
Magnetic field	10
Radiometrics	11
Synthesis of data for the northern coastal area	11
CONCLUSIONS	11
REFERENCES	12

FIGURES

1. Geology of northeast Tasmania	<i>at end</i>
2. Aeromagnetic surveys of the NETGOLD areas	<i>at end</i>
3. Gravity station distribution, northeast Tasmania	<i>at end</i>
4. Gravity of northeast Tasmania	<i>at end</i>
5. Magnetics of northeast Tasmania	<i>at end</i>
6. Aeromagnetic data upward continued 1500 m — northeast Tasmania	<i>at end</i>
7. Two dimensional gravity and magnetic model from Port Sorell to Boulder Point.	<i>at end</i>
8. Two dimensional gravity and magnetic model from Port Sorell to Boulder Point with the aeromagnetic data upward continued 1500 m....	<i>at end</i>
9. Two dimensional gravity and magnetic model from Elizabeth Town to Scamander	<i>at end</i>
10. Two dimensional gravity and magnetic model from Elizabeth Town to Scamander with the aeromagnetic data upward continued 1500 m....	<i>at end</i>
11. Residual gravity anomaly, Fingal NETGOLD area	<i>at end</i>
12. Residual gravity anomaly, Fingal NETGOLD area. Polygons from the 1:250 000 digital geology and primary gold mineralisation shown.	<i>at end</i>
13. Residual magnetic intensity, Fingal NETGOLD area	<i>at end</i>
14. Automatic gain control filtered residual magnetic intensity, Fingal NETGOLD area	<i>at end</i>
15. Residual magnetic intensity, Fingal NETGOLD area. Polygons from the 1:250 000 digital geology and primary gold mineralisation shown	<i>at end</i>
16. Radiometric total counts, Fingal NETGOLD area. Polygons from the 1:250 000 digital geology shown	<i>at end</i> <i>at end</i>
17. Radiometric element colour composite, Fingal NETGOLD area. Polygons from the 1:250 000 digital geology shown	<i>at end</i>
18. Radiometric ratio colour composite, Fingal NETGOLD area. Polygons from the 1:250 000 digital geology shown	<i>at end</i>
19. Two dimensional gravity and magnetic model of the Mathinna area	<i>at end</i>
20. Two dimensional gravity and magnetic model of the Mathinna area with the magnetic data upward continued 1500 m	<i>at end</i>
21. Two dimensional gravity and magnetic model of the Mt Victoria area	<i>at end</i>
22. Two dimensional gravity and magnetic model of the Mt Victoria area with the magnetic data upward continued 1500 m	<i>at end</i>
23. Two dimensional gravity and magnetic model of the Mt Victoria area with Mathinna Group rocks replacing concealed granodiorite	<i>at end</i>

24. Residual gravity anomaly, NETGOLD northern coastal area	<i>at end</i>
25. Residual gravity anomaly, NETGOLD northern coastal area. Polygons from the 1:250 000 digital geology and primary gold mineralisation shown	<i>at end</i>
26. Residual magnetic intensity, NETGOLD northern coastal area	<i>at end</i>
27. Automatic gain control filtered residual magnetic intensity, NETGOLD northern coastal area. Linear features shown in white	<i>at end</i>
28. Automatic gain control filtered residual magnetic intensity, NETGOLD northern coastal area. Polygons from the 1:250 000 digital geology and primary gold mineralisation shown	<i>at end</i>
29. Residual magnetic intensity, NETGOLD northern coastal area. Polygons from the digital geology and primary gold mineralisation shown	<i>at end</i>
30. Radiometric total counts, NETGOLD northern coastal area. Polygons from the 1:250 000 1:250 000 digital geology shown	<i>at end</i>
31. Radiometric element colour composite, NETGOLD northern coastal area. Polygons from the 1:250 000 digital geology shown	<i>at end</i>
32. Radiometric counts, NETGOLD northern coastal area. Polygons from the 1:250 000 digital geology shown	<i>at end</i>

Abstract

Northeast Tasmania is the major gold-bearing province of the State, with an estimated total production of 54 tonnes of gold. As part of the NETGOLD project, high-resolution aeromagnetic and in-fill reconnaissance gravity data were acquired and have been combined with the pre-existing data sets. This report describes the main features of the regional gravity and magnetic fields, concentrating on the geophysical characteristics of areas of known gold mineralisation. The potential of high-resolution magnetic data to define favourable structural sites for mineralisation is also discussed.

The residual gravity field in northeast Tasmania is dominated by large negative granitoid-related anomalies in the east and by positive anomalies due to a number of sources in the west. The gravity field defines the subsurface distribution of low density granitic rocks. The Lisle–Golconda area is the only region in northeast Tasmania where there is a clear spatial association between sites of gold mineralisation and granitic rocks.

The regional magnetic field shows widespread high-frequency anomalies related to outcropping Jurassic dolerite and Tertiary basalt. Ultramafic rocks crop out west of Beaconsfield, producing a large positive anomaly. The broad West Sandy Cape anomaly is also interpreted to result from ultramafic rocks at depth. The Mathinna Group rocks are generally weakly magnetic with a number of isolated strongly magnetic zones, some of which are spatially associated with gold mineralisation. Image analysis of the high resolution magnetic data shows low-amplitude high-frequency anomalies that relate to lithological and structural variations in the Mathinna Group rocks. Many of these subtle features have not been identified by existing regional geological mapping but may define structures localising mineralising fluids.

High-resolution aeromagnetic data provide a good basis for defining areas of higher prospectivity for detailed exploration using geophysical, geochemical and structural mapping techniques. Detailed gravity measurements have the potential to assist structural interpretation in areas of interest.

INTRODUCTION

The generalised geology of northeast Tasmania is shown in Figure 1. East of the River Tamar the oldest rocks belong to the Mathinna Group, a sequence of Ordovician to Devonian quartz-lithic to pelitic turbidites which have undergone low-grade regional metamorphism. Outcrop is generally poor and the rocks are largely unfossiliferous; as a result the stratigraphy is not well defined. The Mathinna Group has been affected by one main regional deformation which produced moderate to tight folding with fold axes trending NNW to NW. Middle Devonian granitoids of the Blue Tier and Scottsdale Batholiths intruded the Mathinna Group, producing narrow contact metamorphic aureoles. Permo-Triassic sediments unconformably overlie the granites and the Mathinna Group. There are widespread intrusions of Jurassic dolerite, particularly in the west and south of the area, and extensive areas of Tertiary basalt flows and sediments. Much of the northern coastal plain is covered by Quaternary sediments.

West of the River Tamar the oldest rocks are the Proterozoic sediments found in the Badger Head area and also approximately 10 km south of Deloraine. Near Beaconsfield sediments of Cambrian age crop out adjacent to a northerly-trending body of Cambrian ultramafic rocks with a mapped strike extent of about six kilometres. Ordovician sediments, including limestone, crop out within this area. There are no mapped Mathinna Group rocks or granitoids but the geology of the post-Devonian rocks is similar to that east of the Tamar.

Williams (1979) formalised the term Tamar Fracture System based on a presumption that the areas of contrasting geology east and west of the River Tamar were brought into juxtaposition by mega-shear. There is no geophysical evidence for such a structure at this position (Leaman, 1994; Wellman, 1989) and Leaman (*loc. cit.*) states that "at best, it (the Tamar Fracture System) can only describe some post-Carboniferous pull-apart effects and does not convey the most likely structure of the underlying crust". Leaman (1992a) accounted for the 'terrane' change by suggesting a complex frontal thrust system with transport from the northeast. Powell *et al.* (1993) also suggest a thrust relationship, based on structural mapping of the Mathinna Group in the Pipers River area.

Before 1993 the geophysical coverage of northeast Tasmania was somewhat restricted. The Australian Geological Survey Organisation (AGSO) acquired aeromagnetic data over the area in 1985/86 along east-west flight lines 1500 m apart as part of the state coverage. The terrain clearance was highly variable. There were also a number of isolated aeromagnetic surveys flown for exploration companies, and these showed that there was magnetic character associated with the Mathinna Group rocks (Leaman, 1987; Leaman, 1990). The Mineral Resources Tasmania gravity data base had good reconnaissance coverage over the northern third of the area and in the Fingal region but had only sparse coverage elsewhere.

As part of the NETGOLD project it was decided to improve the geophysical coverage in the main areas of gold mineralisation by collecting both aeromagnetic and gravity

data. Four new blocks were flown to give a coverage with a line spacing of 500 m or less over the areas shown on Figure 2. The Fingal, Mt Horror and Pipers River areas were flown with 200 m spaced east-west lines and 400 m spaced north-south lines, while the Weymouth-Cape Portland area was flown with a 400 m square mesh. Two accurately-levelled gravity traverses were read across the main gold belt, one near Mathinna and the other near Mt Victoria, and an extensive reconnaissance coverage was obtained over the surrounding areas. Figure 3 shows the final gravity coverage. The gravity data were fully corrected (including terrain corrections) and are presented in this report in residual Bouguer anomaly form calculated using the 1991 version of the Tasmanian regional gravity field (MANTLE91) of Leaman and Richardson (1989).

Bottrill *et al.* (1992) examined the distribution and characteristics of primary gold mineralisation in northeast Tasmania and concluded that gold veins commonly occur in one major belt and several minor belts, usually with a NNW or less commonly a northeast trend.

REGIONAL OVERVIEW

Gravity field

At a regional scale the residual gravity field (fig. 4) is dominated by extensive granitoid-related negative anomalies east of Scottsdale. The steep west-east gradient at about 547 000 mE passes through the Scottsdale Batholith and marks the boundary between low density granites and adamellites to the east and more dense granodiorites and Mathinna Group rocks to the west. The negative anomaly centred at 555 000 mE, 5 404 000 mN is located in an area of poor data coverage at Ben Lomond and must be treated with caution. Other major negative features include the Cainozoic Boobyalla Sub-basin northwest of Gladstone (Moore *et al.*, 1984; Leaman and Symonds, 1975), the Tamar Graben (Leaman *et al.*, 1973) and the Longford-Cressy Basin (Longman and Leaman, 1971). Leaman *et al.* (1973) interpreted the negative anomalies near Lilydale (501 700 mE, 5 429 000 mN) and Nunamara (530 000 mE, 5 417 000 mN) as lying along an axis of light (2.63 t/m^3) arenaceous Mathinna Group sediments, and the negative anomaly southeast of Weymouth (525 000 mE, 5 450 000 mN) as resulting from a synclinorium of light (2.57 t/m^3) Mathinna Group sediments. Recently acquired physical property data indicate that the Mathinna Group sediments have a density in excess of 2.70 t/m^3 , suggesting the need to modify this interpretation. The small negative anomalies near Jetsonville (540 000 mE, 5 449 000 mN) correspond to filled Tertiary valleys (Leaman *et al.*, 1973) and are partially obscured by the gradient on the western edge of the major granitoids.

The most prominent positive residual gravity anomalies are located within the western half of the area. The largest of these extends about 50 km south from the Badger Head-Port Sorell area and is interpreted by Leaman (1992a) as being produced by a thrust slice of Cambrian volcanic rocks. The fact that this anomaly extends across the northern half of the mapped Precambrian rocks at Badger Head suggests that the Precambrian sequence thins significantly to the north and is underlain by dense Cambrian volcanic rocks (Leaman *et al.*,

1973). The major positive feature at Stony Head was interpreted by Leaman *et al.* (1973) as resulting from heavy (2.75 t/m^3) Mathinna Group rocks or granodiorite at shallow depth. The northwest-trending positive anomaly south of Deloraine (463 000 mE, 5 395 000 mN) corresponds to mapped Precambrian, Cambrian and Ordovician rocks. The positive anomalies at Mt Arnon (513 000 mE, 5 403 000 mN) and Westwood (500 000 mE, 5 407 000 mN) correspond to mapped dolerite and almost certainly represent major feeders. Longman and Leaman (1971) interpreted the Mt Arnon anomaly as a feeder. The two relative positive anomalies near Gladstone (570 000 mE, 5 470 000 mN; 590 000 mE, 5 470 000 mN) suggest a significant thickness of Mathinna Group rocks (Leaman and Symonds, 1975). The relative positive anomaly on the eastern side of Anderson Bay (550 000 mE, 5 467 000 mN) is also probably Mathinna Group sourced.

The main Mangana–Lyndhurst gold belt follows a broad gravity high between the Scottsdale and Blue Tier Batholiths. Roach (1992a) interpreted a maximum thickness of 2.6 km of Mathinna Group materials from two-dimensional gravity and magnetic models.

Magnetic field

The combined aeromagnetic data set for northeast Tasmania shows a number of features that are readily correlated with the mapped outcrop of Jurassic dolerite and Tertiary basalt, shown by the hatched and stippled areas on Figure 5. Much of the dolerite is comparatively thin, as evidenced by the subdued anomalies in areas of outcrop. The dolerite feeders, although not always clearly delineated, show as areas of higher-amplitude positive anomalies. The large northwest–southeast elongated positive anomaly over the Longford–Cressy Basin (505 000 mE, 5 390 000 mN) is sourced mainly by dolerite at depth (Longman and Leaman, 1971). The high-amplitude anomaly west of Beaconsfield (480 000 mE, 5 440 000 mN) is associated with Cambrian ultramafic and mafic rocks and occurs at the intersection of several major magnetic linears (fig. 5). The magnetic low immediately southwest of and adjacent to the Beaconsfield anomaly may be related to a thicker part of the Precambrian Badger Head Block; the gravity low (fig. 4) and the magnetic high are complementary.

The large positive magnetic anomaly south of West Sandy Cape (525 000 mE, 5 460 000 mN) consists of a major low-frequency anomaly due to a deep source overprinted with higher frequency northwest-trending anomalies produced by the Mathinna Group rocks (Feature 12 on fig. 5) and irregular anomalies due to Tertiary Basalt. The offshore positive anomalies near Waterhouse Point (545 000 mE, 5 485 000 mN) and Musselroe Bay (605 000 mE, 5 485 000 mN) are of unknown origin. It is possible that they are basalt sourced but the areal extent and amplitude are unlike other basalt anomalies, suggesting perhaps a deeper seated dolerite source. The Boobyalla Sub-basin appears as a broad magnetic high with a number of isolated, presumably basalt sourced, higher amplitude anomalies.

The following magnetic features are identified on Figure 5:

Feature 1: *The Pyengana Pluton*

This granodiorite body has two distinct components. The first has an average magnetic susceptibility of 8×10^{-3} SI and produces the observed positive anomalies. The other component has a susceptibility of 0.22×10^{-3} SI, closer to the value of most of the other granitoids and the Mathinna Group (Roach, 1992a).

Feature 2: *The Lisle Granodiorite*

This granodiorite has components with low (0.2×10^{-3} SI) and high susceptibility (9×10^{-3} SI) (Roach, 1992b).

Feature 3: *The Mt Stronach Area*

No magnetic susceptibility measurements have been made. This granite is associated with molybdenum and tin mineralisation.

Feature 4-12: *Mathinna Group related anomalies*

Early measurements of magnetic susceptibility made on the Mathinna Group suggested that the rocks were of low susceptibility. Roach (1992a) gives an average value for the Mathinna–Alberton area of 0.15×10^{-3} SI. Further work by Roach (1992b) at Lisle and Gladstone showed Mathinna Group rocks with susceptibilities of up to 6×10^{-3} SI and recent measurements of drill core from near Hogans Road (Brooks Creek DDH, 583 550 mE, 5 414 350 mN) gave susceptibilities of up to 40×10^{-3} SI. The magnetic susceptibility of the Mathinna Group in the drill hole varies rapidly, with changes of two orders of magnitude in ten centimetres.

When viewed on the regional data set (fig. 5) with a 250 m grid mesh, the magnetic anomalies from the Mathinna Group sources are commonly broad (10+ kilometres wavelength) and of low amplitude (typically, several tens of nanoteslas). On the high-resolution data sets (fig. 13 and 26) with a 50 m grid mesh and low terrain clearance, areas of magnetic Mathinna Group appear as high-frequency north to northwest-trending anomalies reflecting the general strike direction. Folding and faulting of the Mathinna Group rocks are clearly apparent in some areas.

To provide a view of the major magnetic features the regional magnetic data were upward continued by 1500 m (fig. 6a, b). The effect of increased source distance is to attenuate near-surface and short wavelength anomalies. As expected the major features previously discussed are apparent in the continued image, and the broad Mathinna Group sourced anomalies have, for the most part, become more pronounced. The main areas of dolerite south and west of the Tamar Valley have a sharp cut-off to the northeast along a northwest-southeast trending linear. An additional feature not readily apparent on Figure 5 or 6a, but visible on Figure 6b is a north-south linear at 535 000 mE.

The interpreted magnetic linears shown on Figure 5 trend within about 45° of north-south. The east-west flight direction, large flight line spacing, and terrain clearance variations in the AGSO data set act to mask the presence of geological features with an east-west trend. Only the more clearly defined linear features are shown.

In the southwestern part of the area the linear features are related either to dolerite intrusions or to the ultramafic body near Beaconsfield. Within the remainder of the area most of the linears are related to Tertiary basalt or lithology changes within the Mathinna Group. The major NNW-trending linear (L1 on fig. 5) marks the eastern boundary of the Fingal Tier dolerites, the position of Catos Dyke, and the eastern margin of the Mathinna Group at feature 7 (fig. 5). Existing data does not indicate whether linear L2 joins either linear L3, along the South Esk Valley, or linear L4 which marks the western boundary of the Mathinna Group in the Ansons Bay and Mt William areas. In the Ringarooma Bay area a northwest-trending feature marks the southwestern margin of the Boobyalla Sub-basin and is sub-parallel to several linears on Waterhouse Point which are interpreted as probable dolerite dykes.

Known gold mineralisation in the main gold belt from Mangana to Alberton falls within a region of essentially non-magnetic Mathinna Group rocks. Further to the north the mineralisation at Lyndhurst and Warrentinna is located on the eastern margin of the regional West Sandy Cape anomaly. Gold mineralisation at Hogans Road, northeast of Mathinna, and to the northeast of Gladstone falls on magnetic anomalies in areas of Mathinna Group outcrop. Mineralisation in the Lisle-Golconda area lies on the broad southern margin of the West Sandy Cape anomaly. Some deposits in this area are spatially associated with anomalies due to magnetic granodiorite which crops out at Lisle, while others occur in non-magnetic areas. The known mineralisation at Lefroy and Back Creek falls on the margin of a broad regional anomaly. Deposits at Beaconsfield lie in a magnetically quiet zone to the east of the ultramafic anomaly.

Synthesis of the data sets

Regional interpretation is assisted by comparison of the gravity (fig. 4) and magnetic (fig. 5) maps. In the western half of the area several of the major dolerite feeders are reflected in both the gravity and high-level magnetic anomaly (fig. 6) fields. The Longford-Cressy Basin shows as a negative gravity feature, due to the extensive thickness of Tertiary sediments, and as a positive magnetic anomaly due to the presence of dolerite at depth. In the Badger Head Precambrian block the gravity and magnetic anomalies are complementary — the gravity high lies entirely north and west of the magnetic low. This is interpreted as resulting from a greater thickness of Precambrian rocks in the southern part of the Badger Head Block. The West Sandy Cape magnetic high corresponds to a slight gravity low but there is a difference in the source depths. There is a close correlation between positive gravity and negative magnetic anomalies in the Stony Head area.

At the eastern side of the area there is a correspondence between the gravity and magnetic anomaly of the northeastern part of the Pyengana Pluton. The main southwestern part, although having a distinct magnetic anomaly, has no obvious gravity anomaly due to the small density contrast with the surrounding Mathinna Group rocks. The Boobyalla Sub-basin has a negative gravity anomaly due to the thick layer of low density sediments, and a positive magnetic anomaly resulting from dolerite-derived conglomerate and possibly basalt flows.

Quantitative interpretation

There are a number of recent structural models for northwest and central northern Tasmania (Leaman, 1992a; Elliott *et al.*, 1993; Woodward *et al.*, 1993; Powell and Baillie, 1992). These models show thin-skinned style deformation involving stacking of thrust slices of Precambrian basement, Cambrian, Ordovician and Devonian rocks above a northeast-dipping detachment. To test these models is beyond the scope of this report. The concept of thin-skinned deformation was considered in developing the models presented here.

Two representative profiles (Lines 1 and 2 on Figures 1, 4 and 5) were selected to examine the structure of northeast Tasmania. Line 1 crosses the Badger Head block, the ultramafic rocks at Beaconsfield, the Tamar Valley and the West Sandy Cape magnetic anomaly. Line 2 crosses the Longford-Cressy Basin and the Tamar Valley, and ends north of Scamander. The models for both lines are somewhat simplified, with no attempt to model areas of 'neutral density and magnetisation'. The physical properties used in the models were compiled from Leaman (1986; 1988; 1992a) and Roach (1992a, b) and are summarised in Table 1.

Line 1 (fig. 7)

The eastern end of this line passes across the Scottsdale and Blue Tier Batholiths. The granite thickness decreases from 8 km at the eastern end of the section to about 6 km at the western margin of the granite of the Scottsdale Batholith. A granodiorite component of the Scottsdale Batholith extends about 3 km west of the main granite margin. The section crosses the northern extension of the Lisle granodiorite at about 70 000 m. The Mathinna Group rocks have a thickness of about 2000 m in the Gladstone area but shelve rapidly to the west to a thickness of 100 to 200 m over the granite. In the Tamar Valley region the Mathinna Group has a maximum thickness of about 2200 metres. There is a shallowly east-dipping slice of ultramafic rocks from 42 000 m extending to a depth of about 8000 metres. In the Beaconsfield area there is a near-vertical ultramafic body flanked on the east by thin wedges of Cambrian volcanic rocks and on the west by Precambrian rocks of the Badger Head block. The Cambrian volcanic rocks which crop out in the Port Sorell area are modelled to underlie the Badger Head block. This is consistent with the interpretation of Leaman *et al.* (1973). The calculated gravity profile from the model closely matches the observed gravity data along the entire line but the magnetic profile has been poorly matched by the model west of 38 000 metres.

To provide a check on the model for the large magnetic sources the magnetic profile was calculated for a survey height of 1600 m (100 + 1500 m) and compared to the upward continued magnetic data shown in Figure 6 (fig. 8). The agreement is good east of 38 000 metres. The large differences at 10 000 m and 30 000 m show that there are large deep magnetic sources missing from the model, possibly suggesting the presence of further ultramafic bodies.

Line 2 (fig. 9)

The main features on this line are the gravity low, and corresponding magnetic high, over the Longford–Cressy Basin (25 000 m) and the steep west-east gradient over the western edge of the granite (80 000 m). There is a long-wavelength increase in the magnetic field to the west of 60 000 m which is only obvious on the observed data set west of the Longford–Cressy Basin (fig. 9) but is clearly visible on the upward continued data (fig. 10). The maximum thickness of Mathinna Group rocks on this section is 2300 m and there are two bodies of Mathinna Group materials of higher susceptibility (6.0×10^{-3} SI) at 75 000 m and 98 000 m corresponding to features 10 and 11 (fig. 5) respectively. The dolerite feeder on the eastern side of the Longford–Cressy Basin has a magnetic susceptibility of 60×10^{-3} SI. The western margin of the basin includes slices of Cambrian volcanic and ultramafic rocks. The observed gravity and magnetic data are both well matched by the profiles calculated from the model. The magnetic profile calculated from the model for a survey height of 1650 m (150 + 1500 m) (fig. 10) agrees well with the upward-continued magnetic data.

Interpretation of the magnetic and gravity data along Lines 1 and 2 shows a maximum thickness for the Mathinna Group of 2300 metres. The base of the granite varies from a depth of less than 6000 m in the centre of Line 1 to over 10 000 m at the eastern end of Line 2. The West Sandy Cape magnetic anomaly is sourced by strongly magnetic materials, interpreted as ultramafic rocks, at a depth of 3000–6000

metres. On the western ends of both lines, steeply-dipping fault zones are associated with east-dipping slices of Cambrian and Precambrian rocks.

THE NETGOLD AREAS**Fingal Area**

The Fingal Area includes the Mangana–Alberton gold belt, Golden Ridge, and the Scamander area. The aeromagnetic coverage comprises three surveys — the Alberton survey with east-west lines spaced 500 m apart; the Mathinna survey with 150 m north-south lines; and the Fingal survey with east-west lines spaced 200 m apart. The variation in flight line direction and spacing means that there is potential for biasing magnetic and radiometric features by enhancing trends approximately perpendicular to the flight direction. This bias must be considered when viewing the aeromagnetic data, particularly in image form, as apparent changes in trend may occur across survey boundaries. The gravity coverage is generally restricted to areas of vehicular access where a nominal 1 km spacing between stations was achieved. There is a higher station density in the vicinity of the Golden Gate mine at Mathinna and also along approximately east-west lines near Mathinna (Line M1 on fig. 11) and Mt Victoria (Line M2 on fig. 11).

Gravity field

The residual gravity field (fig. 11) is dominated by a large north to NNW-trending relative positive anomaly. This

Table 1

Physical properties used during modelling

	Lithology	Abbreviation	Density (t/m^3)	Susceptibility $\times 10^{-3}$ SI
Tertiary	Sediments	Ts	2.00	0
	Basalt	Tb	2.85	>10
Jurassic	Dolerite	Jdl	2.80	10 (higher for granophyre)
Permian	Sediments	Ps	2.40	0
Blue Tier Batholith	Granite	Bgr	2.61	0.05
	Granite (St Helens)	Bsh	2.58	0.05
Pyengana Pluton	Granodiorite	Pgd	2.71	0.22
		Pgm	2.75	8.0
Scottsdale Batholith	Granite	Sgr	2.62	0.12
	Tombstone Creek Pluton	Stc	2.58	0.20
	Granodiorite	Sgd	2.71	0.20
		Sgm	2.71	9.0
Devonian	Dolerite	Ddl	2.80	6.0
Mathinna Group	Metasediments	Sms	2.74	0.15
		Sml	2.75	6.0
		Smm	2.75	30.0
Ordovician	Sediments	O	2.60	0
Cambrian	Volcanic rocks	Cv	2.85	10
	Sediments	Cs	2.75	0
	Ultramafic rocks	Cu	2.67	75
Precambrian		Pc	2.67	0

anomaly lies predominantly within an area of Mathinna Group rocks but is more restricted than the mapped Mathinna Group outcrop. The northern end of the anomaly is terminated by a northeast-trending feature passing through 570 000 mE, 5 430 000 mN parallel to a negative anomaly linking the Mt Paris Mass and the Tombstone Creek Pluton. The southwestern margin of the positive anomaly terminates at a linear feature trending NNW from Tower Hill (570 000 mE, 5 400 000 mN) which also marks the southwestern boundary of the Tombstone Creek Pluton.

The similarity in density of the Mathinna Group rocks and most of the granodiorites means that they cannot be discriminated using the gravity method. An example of this is the Pyengana Pluton, where the southwestern part of the pluton (575 000 mE, 5 423 000 mN) is gravimetrically indistinguishable from the adjoining Mathinna Group materials (fig. 12). The northeastern section of the pluton has a positive density contrast compared to the surrounding granites and shows clearly as a relative positive anomaly (580 000 mE, 5 430 000 mN).

The large negative anomaly adjacent to the coast may be partly due to an artefact of the regional gravity model used to produce the residual anomaly but it also corresponds to major low-density granites and adamellites. Several granodioritic bodies show as positive anomalies within this area, including the Gardens Pluton and an isolated part of the Georges River granodiorite west of St Helens (593 000 mE, 5 430 000 mN), suggesting that these bodies are significantly thicker than other mapped granodioritic bodies within this area. The granite at Storys Creek (361 000 mE, 5 382 000 mN) has a distinct negative residual gravity anomaly. North of Ben Lomond (5 550 000 mE, 5 403 000 mN) there is a small negative anomaly but there is insufficient data to accurately define either the southern margin of this anomaly or the east-trending positive anomaly which crosses the southern part of the Ben Lomond Plateau.

The known primary gold mineralisation, with the exception of that at Golden Ridge, lies predominantly within the major positive anomaly (fig. 12). The gold belt between Mathinna and New River is approximately along the axis of the positive anomaly and appears to lie above the region of greatest thickness of Mathinna Group rocks. There is a break in the gold belt southwest of Mt Victoria (586 000 mE, 5 419 500 mN) corresponding to a small SSW-trending negative anomaly defined by three independent gravity stations. The northern end of the belt terminates abruptly at New River on the southeastern flank of the gravity low joining the Tombstone Creek Pluton with the Mt Paris Mass.

If the combination of a positive relative gravity anomaly and coincident Mathinna Group rocks is regarded as one possible criterion for the location of primary gold mineralisation then the area between Mathinna and Fingal must be regarded as prospective. To confirm or discount this proposition further detailed data acquisition and interpretation is required for accurate determination of the structural setting. The possibility of granodiorites rather than Mathinna Group materials producing the positive anomaly must also be considered.

Magnetic field

Qualitative interpretation of the aeromagnetic data for the Fingal area (fig. 13 and 15) should be conducted in conjunction with the 1:250 000 scale NETGOLD geological map (McClenaghan and Calver, 1994). Areas of Jurassic dolerite and Tertiary basalt correlate well with high-frequency positive anomalies, and it appears that there may be a small area of unmapped dolerite at 567 000 mE, 5 398 000 mN. The other easily correlated feature is the Pyengana granodiorite, which also shows as a strong positive anomaly. The southwest part of the Pyengana granodiorite is a composite body with strongly magnetic and effectively non-magnetic components which are apparent as magnetic lows.

The Mathinna Group rocks are variably magnetic, and subtle northwest-trending features marking lithological variations are visible in all areas. West of Mathinna (565 000 mE, 5 410 000 mN), near Alberton, and in the Golden Ridge (583 000 mE, 5 413 000 mN) area the Mathinna Group rocks are strongly magnetic (30×10^{-3} SI) but elsewhere they appear to exhibit other levels of magnetisation. In the Mathinna area and between Catos Dyke and Scamander, the Mathinna Group materials are effectively non-magnetic (0.15×10^{-3} SI), while the remaining areas, with the exception of west of Tower Hill (565 000 mE, 5 400 000 mN) and along the South Esk Valley (575 000 mE, 5 385 000 mN) are slightly magnetic.

The valleys of the South Esk River and Tower Rivulet have narrow, often braided, high-frequency positive anomalies that are interpreted to be sourced by dolerite boulder beds, which have been intersected by drilling north of Fingal (J. L. Everard, pers. comm.). There are a number of northeast-striking linear positive anomalies in the Catos Dyke–Falmouth–St Helens area. One of these correlates with a mapped Devonian dolerite dyke near the Great Pyramid Mine (600 000 mE, 5 413 000 mN), and it is probable that the other similar anomalies are also sourced by dolerite dykes. The linear features offset some anomalies (601 000 mE, 5 416 000 mN), truncate others (597 000 mE, 5 412 000 mN), and align with mapped faults (595 000 mE, 5 409 000 mN; 603 000 mE, 5 413 000 mN). Catos Dyke appears as a low-amplitude negative magnetic anomaly.

An automatic gain control (AGC) filter was applied to the data to enhance subtle linear features (fig. 14). An AGC filter is a non-directional form of high pass filter which enhances high and low amplitude features including noise and levelling artefacts. The western and northern parts of the images were derived from the Alberton survey and show prominent east-west features related to mis-levelling of the data. These can be removed by further processing of the located data. A number of linear and curvi-linear features have been highlighted on Figure 14. These predominantly trend northeast and northwest. There are few features on the image that can be attributed to flight line biases. With the exception of features within the Pyengana granodiorite, most north to northwest-trending features terminate against northeast-trending features. In the Pyengana granodiorite the linears are mainly negative, indicating destruction of magnetite. There is evidence for a major northeast-trending fault which truncates a linear at 579 000 mE, 5 395 000 mN and aligns with other discontinuities to the northeast. The

linear on the western side of Catos Dyke is not offset by this fault.

The sites of gold mineralisation from the MIRLOCH database are shown overlayed on the magnetic image in Figure 15. The main gold belt lies along a magnetic low. This is particularly apparent between Alberton and New River, where the belt follows a narrow magnetic low. Further south the magnetic low is broader and the gold occurrences have a greater scatter. In the Mangana area the known primary gold mineralisation lies on the northeastern side of a northwest-trending magnetic high. The other primary gold occurrences are in the Golden Ridge area on the northern part of a positive anomaly attributed to high susceptibility Mathinna Group materials. Areas of potential prospectivity for gold, based on the magnetic data, are within the general magnetic low between Alberton and Fingal and in areas of positive anomalies produced by high susceptibility Mathinna Group rocks such as west of Mathinna.

Radiometrics

The radiometrics total count map (fig. 16) shows four distinct count regimes. Areas of Permo-Triassic sediments, Jurassic dolerite and some Quaternary deposits have generally low total counts. The flood plain, but not the higher terraces, of the South Esk valley north of Fingal, the New River valley and the flood plain of the Tower Rivulet valley all have elevated total count values. The Scottsdale Batholith west of Mt Saddleback, the northern part of Catos Dyke, the Pyengana Pluton and the Scamander Dyke (604 000 mE, 5 415 000 mN) are all areas of high total counts. The Mathinna Group rocks give slightly elevated counts, with a northwest trend visible east of Tower Hill and northwest of Mathinna.

A three-colour composite (K = red, Th = green, U = blue) image (fig. 17) provides discrimination of lithologies. The northern part of Catos Dyke is high in all three elements whereas the southern part, the St Marys Porphyry and the Scamander Dyke, are all high in potassium. Much of the area of Permo-Triassic sediments is high in thorium, low in uranium and of about average value (for this area) in potassium. There is a combined potassium-thorium anomaly north of Tower Hill. Conventional three-colour composite images may mask significant variations in areas of low total counts which appear as dark zones in the image. A three-colour composite ratio image (K/TC = red, Th/TC = green, U/TC = blue) (fig. 18) removes the effects of variations in total count and provides more detailed lithological data, particularly in areas of Permo-Triassic sediments.

The radiometric data is most useful as a mapping tool, particularly for geomorphic mapping, as only the upper metre (approximately) of the ground surface contributes to the recorded counts. The radiometric data clearly maps the distribution of surficial sediments. In areas of Mathinna Group outcrop radiometric anomalies may reflect variations in lithology or possibly alteration.

Quantitative Interpretation

To provide further details of the structural setting of the Alberton-Mangana gold belt two representative

cross-sections have been modelled (Lines M1 and M2, Figures 11 and 13).

(1) Line M1

This line starts on the Scottsdale Batholith south of Ben Nevis, passes along the South Esk Valley north of Mathinna, and terminates at Scamander. The model (fig. 19) has a granitic basement for the entire length. In the absence of any subsurface data confirming the presence of granodiorite in the Mathinna area the section was modelled using Mathinna Group materials only, except where surface mapping showed granodiorite. A comparison of the physical properties of the Mathinna Group materials and the Pyengana Pluton granodiorites (Table 1) shows that the magnetic granodiorite (Pgm) and the magnetic Mathinna Group rocks (Sml) are so similar in properties that in most situations they may be used interchangeably in models.

The section shows a maximum thickness of approximately 2 km of Mathinna Group rocks in the Mathinna area with the thickness decreasing steadily to the east. The shallower Mathinna Group materials are non magnetic, with the exception of a highly magnetic (30×10^{-3} SI) lense at a depth varying from 400 m in the west near the margin of the Scottsdale Batholith to 1100 m approximately 4 km east of Mathinna. There is a layer of less magnetic (6.0×10^{-3} SI) Mathinna Group rocks overlying the granite basement. The gold belt crosses the section at approximately 23 000 metres. There are minor dykes of dolerite in the eastern part of the section. The magnetic profile calculated from the model for a survey height of 1600 m (100 + 1500 m) (fig. 20) agrees well with upward continued magnetic data. A small datum shift is required to match the profiles.

(2) Line M2

This line starts on the Scottsdale Batholith just west of the Tombstone Creek Pluton, passes across the gold belt in an area of historically low prospectivity near Mt Victoria, and ends near Dianas Basin. The line also crosses the Pyengana Pluton. The modelled section (fig. 21) is underlain by granite for the entire length.

The Pyengana Pluton has both magnetic and non-magnetic components, and this model assumes that the magnetic component is underlain by non-magnetic granodiorite. There is a maximum thickness of 3000 m of average susceptibility (0.15×10^{-3} SI) Mathinna Group rocks and the main Alberton-Mangana gold belt crosses the section at approximately 18 000 metres. There is a large negative magnetic anomaly at the western margin of the Pyengana Pluton and this has been modelled as a reversely magnetised body with a susceptibility of -12×10^{-3} SI. The requirement for the presence of this body is somewhat contentious, as the data from the 1989 Alberton survey do not show such a large negative anomaly and have been modelled by Roach (1992a) using only induced magnetisation. Further field work is required to ascertain the cause of this anomaly.

Both the Tombstone Creek Pluton and the St Helens Pluton have been modelled using a density of 2.58 t/m^3

rather than the more usual granite density of 2.61 t/m^3 to match the large negative residual gravity anomalies. A comparison of the magnetic profile calculated from the model for a survey height of 1600 m ($100 \times 1500 \text{ m}$) and the upward continued magnetic data (fig. 22) shows good agreement except over the reversely magnetised body, suggesting that further refinement of the model is required.

To emphasise the possible ambiguity of modelling when both Mathinna Group materials and granodiorite can be used as anomaly sources, this section has been re-calculated after substituting Mathinna Group rocks for the non-outcropping Pyengana granodiorites on the model (fig. 23). There is a slight change in the gravity profile but no visible change in the calculated magnetic profile.

Synthesis of the data for the Fingal area

The primary gold mineralisation, with the exception of Golden Ridge, is predominantly within a positive gravity anomaly and a magnetic low. The width of the gold belt appears to be controlled in part by the width of the magnetic low. The abrupt termination of the belt near Alberton and New River coincides with a negative gravity anomaly joining the Tombstone Creek Pluton and the Mt Paris Mass. The Golden Ridge mineralisation is coincident with a magnetic high sourced by Mathinna Group materials. A comparison of two sections across the gold belt shows that the area of historically low prospectivity near Mt Victoria has predominantly low susceptibility ($0.15 \times 10^{-3} \text{ SI}$) Mathinna Group rocks while the area near Mathinna has susceptibilities of up to $30 \times 10^{-3} \text{ SI}$ at depth.

The areas of highest prospectivity for gold are the coincident gravity high and magnetic low extending SSE from Mathinna, and Mathinna Group sourced magnetic highs similar to those near Golden Ridge. To evaluate this potential will require high-resolution magnetic and gravity surveys to assess and target favourable structural sites for mineralisation.

The Northern Coastal Area

The northern coastal area includes the Back Creek, Lefroy, Golconda, Lisle, Lyndhurst, Mt Horror, Warrentinna and Gladstone goldfields. The aeromagnetic coverage consists of six surveys, the details of which are summarised in Table 2.

Table 2

Aeromagnetic Surveys — NETGOLD Northern Coastal areas

Survey	Date	Details
Lisle	1983	200 m N-S Lines
Lyndhurst	1987	125 m E-W Lines
Gladstone	1987	125 m E-W Lines
Mt Horror	1993	200 m E-W Lines
Pipers River	1993	200 m E-W Lines
Weymouth—Cape Portland	1993	400 m Square Mesh

The effects of different flight line spacing and directions must be considered when viewing the gridded airborne data in image form.

The gravity coverage is generally restricted to stations spaced one to two kilometres apart along vehicle access routes. In the Gladstone area Roach (in prep.) has acquired data with a station density of better than one station per square kilometre as part of an assessment of the structural setting of the Gladstone goldfield.

Gravity Field

The residual gravity field (fig. 24) is dominated by large-scale northeast to northwest-trending features. The Blue Tier and Scottsdale Batholiths produce extensive negative gravity anomalies. The Gardens Pluton extends from The Gardens north to near Gladstone and produces a positive anomaly. Relative positive anomalies correspond to outcropping Mathinna Group rocks in the Gladstone area, between Lyndhurst and Branhholm, south of Bridport, and south of Stony Head.

The large negative anomalies corresponding to the Blue Tier and Scottsdale Batholiths reduce in amplitude but extend to the north coast at Waterhouse Point and Anderson Bay respectively. The negative anomaly associated with the outcropping Musselroe Pluton also extends northwest to the coast.

The relationship between the known primary gold mineralisation and the residual gravity anomaly (fig. 25) is more complex than in the Mathinna area. The extension of the Alberton—Mangana gold belt through Warrentinna, Mt Horror and Lyndhurst follows a NNW-trending gravity high which corresponds to outcropping Mathinna Group rocks. In the Gladstone area the sites of primary gold mineralisation fall in two distinct zones. The mineralisation northeast of Gladstone ($590\ 000 \text{ mE}$, $5\ 474\ 000 \text{ mN}$) occurs in an area of relative positive gravity anomaly corresponding to the zone of Mathinna Group rocks which separate the Blue Tier and Eddystone Batholiths. Mineralisation near Gladstone township occurs within contact metamorphosed Mathinna Group rocks on the northern boundary of the Blue Tier Batholith. The gravity field in this area has a steep gradient due to the major granite-related anomaly to the south.

In the Lisle—Golconda—Denison goldfield Roach (1992b) acquired additional gravity data (not shown on Figures 24 or 25) and found that the mineralisation at both Lisle and Denison occurs near relative negative gravity anomalies. Modelling by Roach (*loc. cit.*) interpreted a pluton beneath the Denison goldfield with a different composition to the granodiorite exposed at Lisle and Golconda. The Back Creek and Lefroy goldfields are in Mathinna Group rocks on a large positive gravity anomaly (the Stony Head anomaly).

Magnetic field

The aeromagnetic images for the northern NETGOLD area (fig. 26 and 29) should be viewed in conjunction with the 1:250 000 NETGOLD geological map (McClenaghan and Calver, 1994). At a regional scale, the data fall into three main areas. The first is an area of low background east of Croppies Point ($551\ 000 \text{ mE}$, $5\ 477\ 000 \text{ mN}$); the second is an area of generally positive anomalies south of West Sandy

Cape, bounded on the western side by a linear feature between Weymouth and Lebrina; and the third is an area of low background between Weymouth and the western boundary of the survey area.

Areas of dolerite are characterised by positive anomalies but areas of basalt show as both high-frequency positive anomalies, indicating either no or slight remanent magnetisation, and high-frequency negative anomalies, indicating reverse remanent magnetisation. There are two linear features, presumably dolerite dykes, trending southeast from Waterhouse Point.

North to northwest-trending linear anomalies occur in areas of Mathinna Group outcrop. These are interpreted as lithological units and are locally parallel to the strikes of the Mathinna Group. In the Gladstone area Leaman (1992b) and Roach (in prep.) examined the high-resolution (125 m line spacing, 60 m terrain clearance) aeromagnetic data and used magnetic marker units within the Mathinna Group to define fold closures and fault-bounded blocks. In the Mt Horror–Branxholm area there are a number of small magnetic features, some of which fall in areas of contact metamorphism and intersect the northwest to NNW-trend of Mathinna Group anomalies.

In the Lisle–Golconda area parts of the Lisle granodiorite are strongly magnetic. Roach (1992b) sampled the granodiorites in this area and found a bimodal distribution of susceptibility with values either less than 0.3×10^{-3} SI or between 4 and 12×10^{-3} SI. A broad magnetic anomaly extends north from the Lisle valley, marking the subsurface extension of the magnetic lithology.

To enhance linear features an image was produced using an automatic gain control filter (fig. 27). This image shows numerous geological features but also highlights major levelling problems in the Lyndhurst data set and minor levelling problems in the Gladstone and Lisle data sets. In common with the Fingal data the predominant direction of the linears is northwest to NNW and NNE to northeast. There are north-trending features in the Gladstone area, some of which are truncated by northwest-trending linears. The folded magnetic units of the Mathinna Group at Gladstone are clearly visible on this image. When compared with the mapped geology of the area (fig. 28) few of the linears can be directly related to mapped geological features. The major feature commencing at 565 000 mE, 5 475 000 mN and extending southeast to 579 000 mE, 5 469 000 mN before turning northeast delineates the southern boundary of the magnetic anomalies associated with Boobyalla Sub-basin.

The known primary gold mineralisation lies predominantly on the flanks of positive magnetic anomalies (fig. 29). By selectively enhancing portions of the image it is possible to examine this relationship in more detail. The mineralisation between Lyndhurst and Warrentinna falls on the flank of a broad anomaly. The Denison goldfield lies at the southern margin of the major West Sandy Cape anomaly. In the Lisle–Golconda area many of the sites of gold mineralisation occur close to magnetic highs sourced by granodiorites (Roach, 1992b). Interference from strong basalt-related anomalies at Lefroy confuses the anomaly pattern but it appears that the deposits lie on a subtle magnetic low. The

known gold mineralisation northeast of Gladstone lies mainly within anticlinal zones defined by the distribution of magnetic units within the Mathinna Group.

Radiometrics

The radiometric total count image (fig. 30) shows the granitoids between Waterhouse Point and Stumpys Bay clearly as high count rate areas. Other areas of high total count are the alluvium in a number of river valleys (e.g. Great Forester River, Brid River, Musselroe River, Ringarooma River) and areas of surficial deposits near Lyndhurst and Gladstone. The Mathinna Group rocks in a number of areas exhibit northwest to NNW-trending features which may be related to variations in lithology.

The three-colour composite image (K = red, Th = green, U = blue) (fig. 31) shows a variation within the coastal area from high potassium count rates in the northeast to lower potassium and higher thorium counts in the western part of the area. There is an area of anomalously low counts visible on both this image and the total count image (fig. 30). This feature has sharp southeastern and northeastern boundaries (520 000 mE, 5 447 000 mN) and may reflect either lithological or structural variations in the Mathinna Group or geomorphological effects. Outcropping basalt in the Branxholm area is characterised by low potassium counts. Element ratio images were not available for this area but separate plots of potassium, thorium and uranium counts (fig. 32) show the variation in relative distribution of these elements across the area.

Synthesis of the data for the northern coastal area

Both the gravity and aeromagnetic data for the northern NETGOLD area show long-wavelength high-amplitude anomalies. These anomalies obscure the subtle features which may be associated with the primary gold mineralisation. The Warrentinna–Lyndhurst extension of the main gold belt lies along a relative positive gravity anomaly but the strong magnetic gradient on the eastern flank of the West Sandy Cape anomaly obscures any subtle magnetic signature. In the Lisle–Golconda area gold mineralisation is spatially associated with granodioritic cupolas which are characterised by low-amplitude negative gravity anomalies and irregular magnetic anomalies.

Additional gravity data is required to refine anomalies in areas of sparse data. Removal of the effects of the long-wavelength magnetic and gravity anomalies is required to enhance the subtle features which may indicate favourable structural sites for gold mineralisation.

CONCLUSIONS

The residual gravity field in northeast Tasmania is dominated by negative granitoid-related anomalies in the east and by positive anomalies due to several different sources in the west. The major east-west gradient in the data passes through the Scottsdale Batholith and marks the boundary between low density granites and adamellites to the east and more dense granodioritic and Mathinna Group rocks to the west.

The regional magnetic data is characterised by widespread high-frequency anomalies due to Jurassic dolerite in the southeast and broader, more subdued anomalies in areas of Mathinna Group and granitoid outcrop. A large positive anomaly is associated with outcropping Cambrian ultramafic rocks west of Beaconsfield, and the broad magnetic high south of West Sandy Cape is interpreted to result from another east-dipping body of ultramafic rocks at depths in excess of 3 km beneath the Mathinna Group and granitoids of the Scottsdale Batholith. High-frequency anomalies east of the main dolerite margin result from isolated bodies of Jurassic dolerite, Tertiary basalt and magnetic lithologies in the Mathinna Group.

Known gold mineralisation does not show a consistent correlation with any one set of geophysical criteria. The main gold belt from Mangana to Lyndhurst falls on a positive residual gravity anomaly which correlates with the mapped extent of the Mathinna Group. Modelling suggests a maximum thickness of 2.3 km of Mathinna Group rocks. This anomaly is truncated to the north of the New River by a negative feature which links the Mt Paris Mass and the Tombstone Creek Pluton. Few mineralised sites are recorded from this zone. Between Mangana and Alberton the sites of gold mineralisation follow a negative magnetic anomaly which is parallel to the trend of bedding in the Mathinna Group and probably reflects a gross variation in lithology. North of Alberton the magnetic field is affected by the regional gradient due to the major West Sandy Cape anomaly, and separation of regional and residual anomalies is required to isolate subtle features which may relate to gold mineralisation.

Gold mineralisation at Lefroy and at Beaconsfield is not associated with any clear geophysical features on a regional scale. In the Lisle–Golconda area mineralisation has a close spatial relationship to granodioritic cupolas which are manifest as low-amplitude negative residual gravity anomalies and, in some areas, as irregular magnetic anomalies. Mineralisation northeast of Gladstone falls in an area of positive residual gravity anomaly. This occupies only a small part of the mapped extent of Mathinna Group rocks, which are interpreted to have a thickness in excess of two kilometres. The mineralisation has a strong structural control, with many of the sites falling within the hinge zones of folds defined by magnetic lithologies in the Mathinna Group. The local trend of quartz veins in this area parallels the trend of faulting, which crosscuts the magnetic units (Roach, in prep.). In the Golden Ridge area gold mineralisation falls mainly within the contact metamorphic aureole of the Haleys New Country Pluton. Magnetic anomalies are associated with some areas of mineralisation, and a major magnetic anomaly related to an irregular zone of magnetite alteration in the Mathinna Group occurs just to the west of Golden Ridge (Roach, in prep.). There is no gravity anomaly which corresponds to this magnetic feature. Previous interpretations of this anomaly and similar features to the west and northwest of Mathinna (Roach 1992a) suggested the presence of granodioritic intrusions. This interpretation needs to be modified in the light of recent petrological and petrophysical studies.

The Mathinna Group rocks are typically weakly but variably magnetic. Lithological and structural variations are present

as low-amplitude high-frequency magnetic anomalies which are apparent in the new NETGOLD magnetic data and existing high-resolution company data. Image processing methods such as automatic gain control filters enhance these anomalies, enabling the definition of structural features which may be important in the localisation of mineralising fluids. These subtle features apparent in the new magnetic data have not been identified by existing regional mapping. The aeromagnetic data provide a good basis for the selection of areas for detailed exploration, including ground geophysical and geochemical methods and detailed structural mapping.

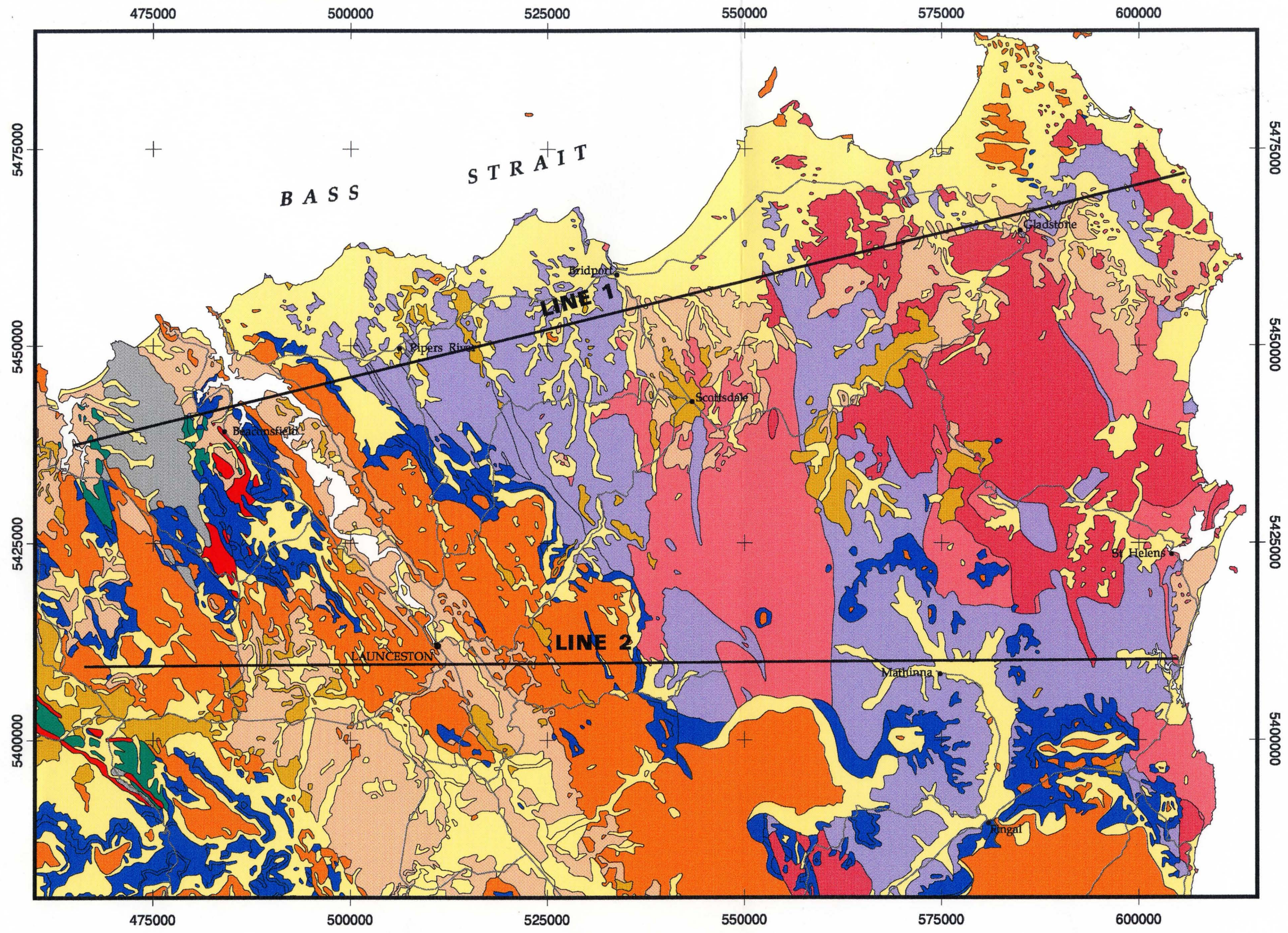
The improved gravity data coverage better delineates the subsurface distribution of low density granites and adamellites. Granodioritic rocks have a higher density than the granites and produce only subtle negative anomalies. Gravity data indicate that there is no clear spatial association between low density granitic rocks and gold mineralisation in the main gold belt from Mangana to Lyndhurst or in the area northeast of Gladstone. The mineralisation sites are located near the crests of broad positive gravity anomalies and are interpreted to be located in the areas of maximum thickness of Mathinna Group rocks. Bodies of dense non-magnetic granodiorite may be present but it is not possible to distinguish these from the gravity data alone. While there is no local relationship between gold mineralisation and granitic intrusions, the entire region is underlain by large volumes of granitic rocks and the possibility of the granites as a heat source or as the regional source of fluids should not be discounted. Gravity data enable the interpretation of Mathinna Group thickness, and detailed measurements have the potential to assist structural interpretation based on the new magnetic data. Infilling the gravity data coverage in the Mangana–Mathinna area and north of Ringarooma are seen as priorities for future work. The subsurface distribution of granodioritic rocks, which are spatially associated with gold mineralisation in the Lisle–Golconda area, is delineated by negative gravity anomalies. Further field work is also required to more accurately define these anomalies.

REFERENCES

- BOTTRILL, R. S.; HUSTON, D. L.; TAHERI, J.; ZAW, K. 1992. Gold in Tasmania. *Bulletin Geological Survey of Tasmania* 70:24–46.
- ELLIOTT, C. G.; WOODWARD, N. B.; GRAY, D. R. 1993. Complex regional fault history of the Badger Head region, northern Tasmania. *Australian Journal of Earth Sciences* 40:155–168.
- LEAMAN, D. E. 1986. Gravity interpretation – west and north-west Tasmania. *Geophysical Report Mt Read Volcanics Project Tasmania* 3.
- LEAMAN, D. E. 1987. *Acquisition report, airborne geophysical surveys EL 34/86 Gladstone. Report for Placeco Australia.* Leaman Geophysics. [TCR 88-2762A].
- LEAMAN, D. E. 1988. Precambrian and Lower Palaeozoic structural relationship of west and north-west Tasmania. *Geophysical Report Mt Read Volcanics Project Tasmania* 7.
- LEAMAN, D. E. 1990. *Aeromagnetic survey, EL 55/83 Mangana. Acquisition report (including preliminary interpretation). Report for Pegasus Gold Australia.* Leaman Geophysics. [TCR 90-3197A].

- LEAMAN, D. E. 1992a. Finding Cambrian keys: an essay in controversy, prospectivity and tectonic implications. *Bulletin Geological Survey of Tasmania* 70:124–148.
- LEAMAN, D. E. 1992b. Gold exploration and the use of magnetic methods in northeast Tasmania. *Bulletin Geological Survey of Tasmania* 70:149–160.
- LEAMAN, D. E. 1994. Geological note: The Tamar Fracture System in Tasmania: Does it Exist? *Australian Journal of Earth Sciences* 41:73–74.
- LEAMAN, D. E.; RICHARDSON, R. G. 1989. Production of a residual gravity field map for Tasmania and some implications. *Exploration Geophysics* 20:181–184.
- LEAMAN, D. E.; SYMONDS, P. A. 1975. Gravity survey of north-eastern Tasmania. *Paper Geological Survey of Tasmania* 2.
- LEAMAN, D. E.; SYMONDS, P. A.; SHIRLEY, J. E. 1973. Gravity survey of the Tamar region, northern Tasmania. *Paper Geological Survey of Tasmania* 1.
- LONGMAN, M. J.; LEAMAN, D. E. 1971. Gravity survey of the Tertiary basins in northern Tasmania. *Bulletin Geological Survey of Tasmania* 51.
- MCCLENAGHAN, M. P.; CALVER, C. R. (comp.). 1994. Netgold 1:250 000 map series. Geology of northeast Tasmania. *Mineral Resources Tasmania*.
- MOORE, W. R.; BAILLIE, P. W.; FORSYTH, S. M.; HUDSPETH, J. W.; RICHARDSON, R. G.; TURNER, N. J. 1984. Boobyalla Sub-basin. A Cretaceous onshore extension of the southern edge of the Bass Basin. *APEA Journal* 24:110–117.
- POWELL, C. MCA.; BAILLIE, P. W. 1992. Tectonic affinity of the Mathinna Group in the Lachlan Fold Belt. *Tectonophysics* 214: 193–209.
- POWELL, C. MCA.; BAILLIE, P. W.; CONAGHAN, P. J.; TURNER, N. J. 1993. The mid-Palaeozoic turbiditic Mathinna Group, northeast Tasmania. *Australian Journal of Earth Sciences* 40:169–196.
- ROACH, M. J. 1992a. Geology and geophysics of the Alberton–Mangana goldfield, northeast Tasmania. *Bulletin Geological Survey of Tasmania* 70:199–207.
- ROACH, M. J. 1992b. Geology and geophysics of the Lisle–Golconda goldfield, northeast Tasmania. *Bulletin Geological Survey of Tasmania*. 70:189–198.
- ROACH, M. J. (in prep). *The regional geophysical and geological setting of gold mineralisation in northeast Tasmania*. Ph.D. thesis, University of Tasmania : Hobart.
- WELLMAN, P. 1989. The relationship between basement in western and northeastern Tasmania, in BURRETT, C. F.; MARTIN, E. L. (ed.). Geology and mineral resources of Tasmania. *Special Publication Geological Society of Australia* 15:459.
- WILLIAMS, E. 1979. Tasman Fold Belt System in Tasmania – Explanatory notes for 1:500 000 structural map of pre-Carboniferous rocks in Tasmania. (Revised ed.). *Department of Mines, Tasmania*.
- WOODWARD, N. B.; GRAY, D. R.; ELLIOTT, C. G. 1993. Repeated Palaeozoic thrusting and allochthoneity of Precambrian basement, northern Tasmania. *Australian Journal of Earth Sciences* 40: 297–311.

[8 April 1994]

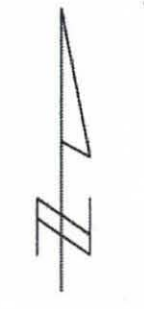


- Legend**
- Quaternary sediments
 - Tertiary sediments
 - Tertiary basalt
 - Jurassic dolerite
 - Permo-Triassic sediments
 - Ordovician - Devonian Mathinna Group sediments
 - Devonian granite
 - Devonian granodiorite
 - Ordovician sediments
 - Cambrian sediments and volcanics
 - Proterozoic sediments

Geology from
Mineral Resources Tasmania
1:500,000 digital geology.

**NE TASMANIA
GEOLOGY**

Figure 1



Scale: 1:500,000
0 10 20 30 40 50
km
Grid: Australian Map Grid, Zone 55.

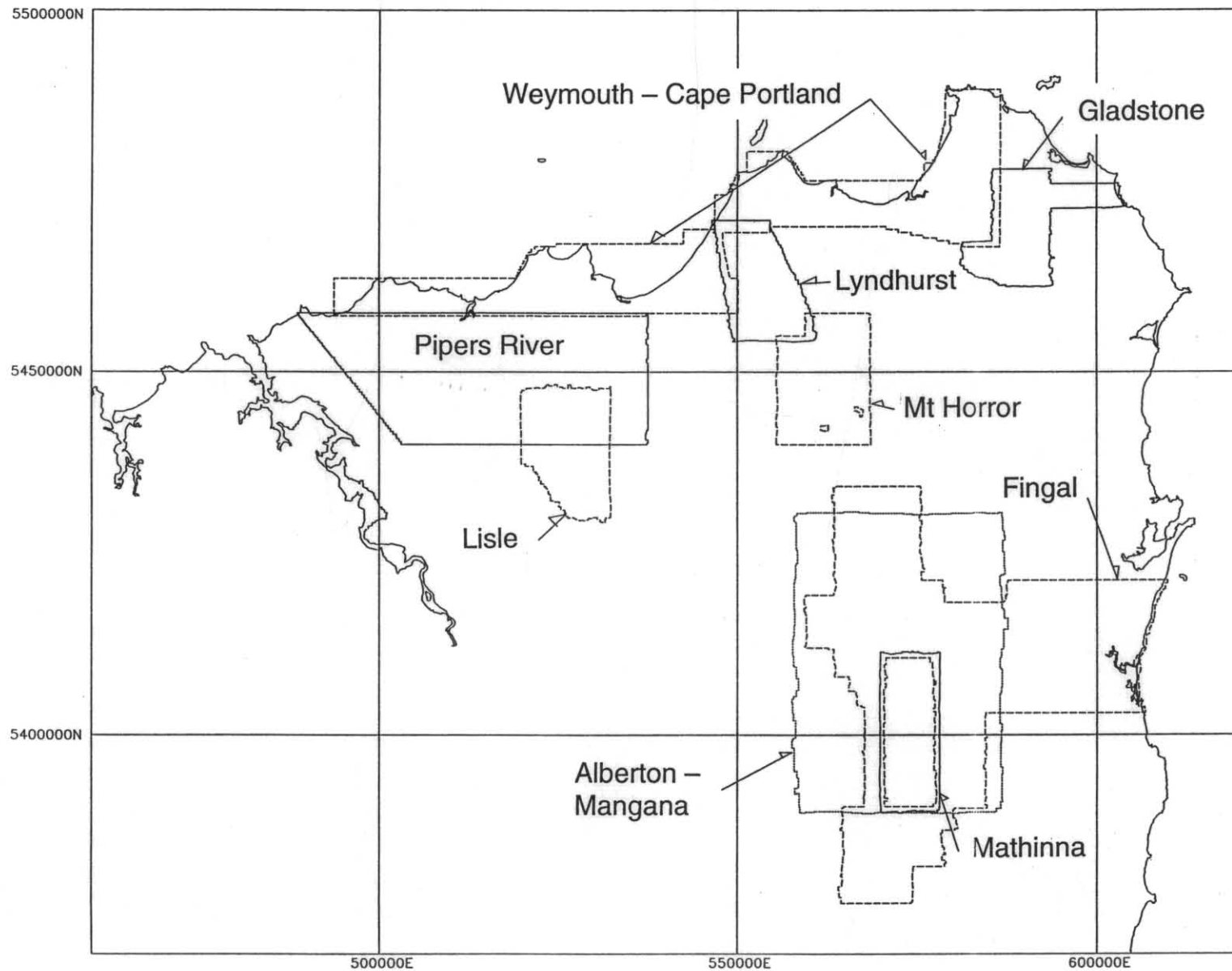


Figure 2. Aeromagnetic surveys of the NETGOLD areas

5 cm

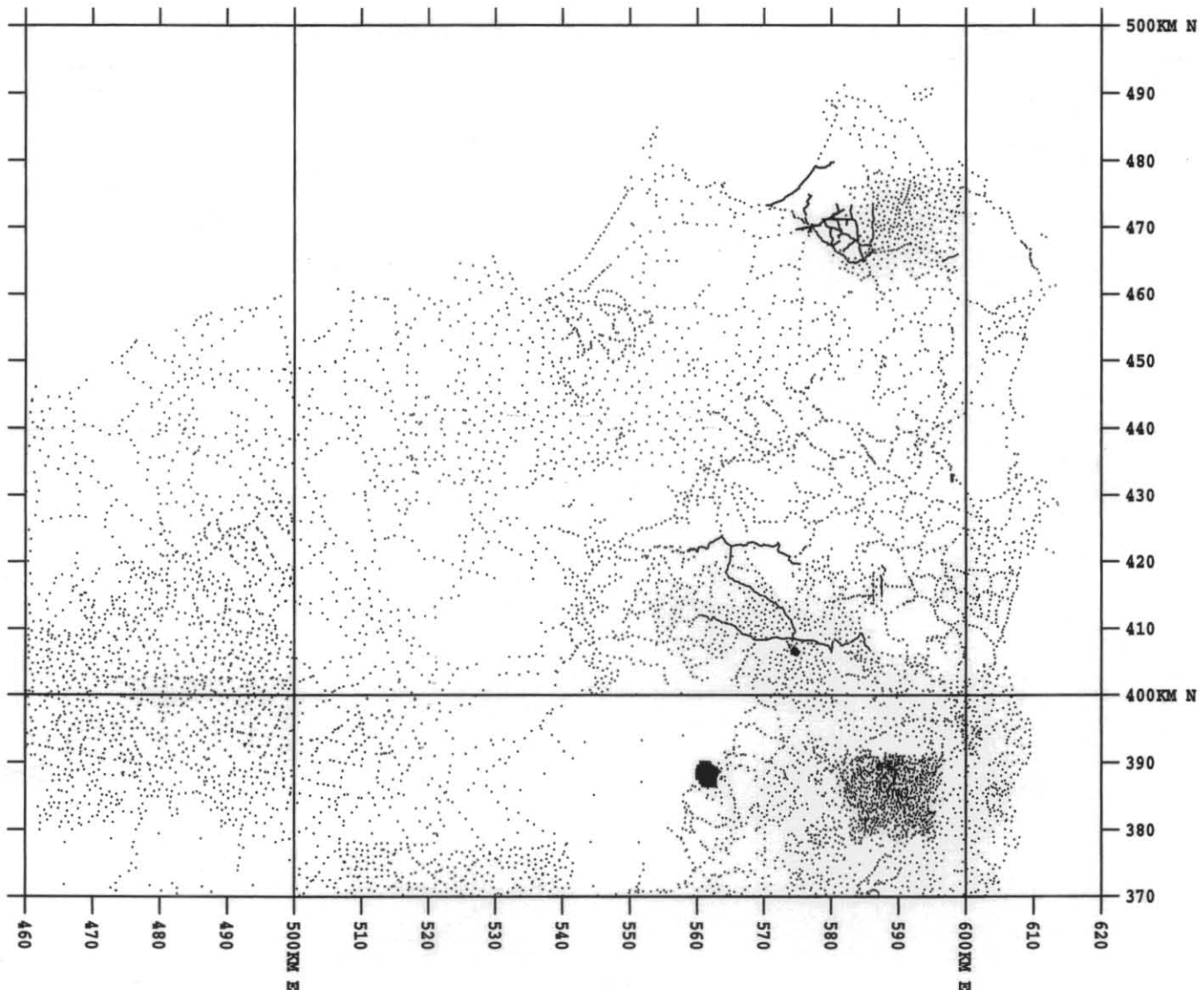
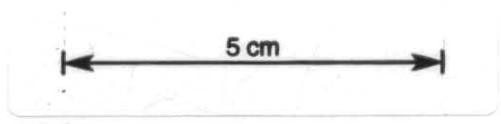
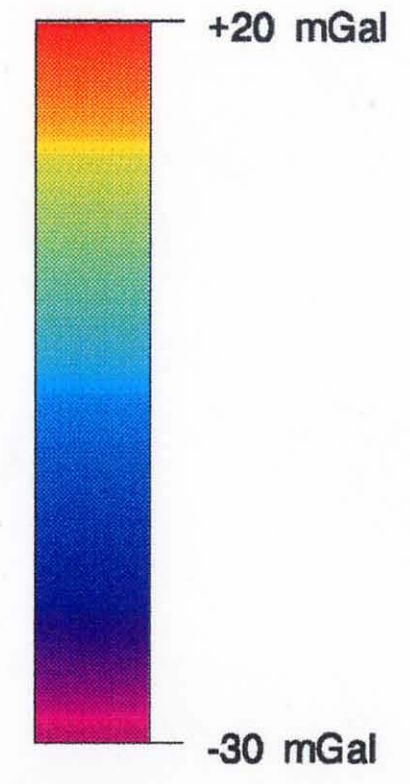
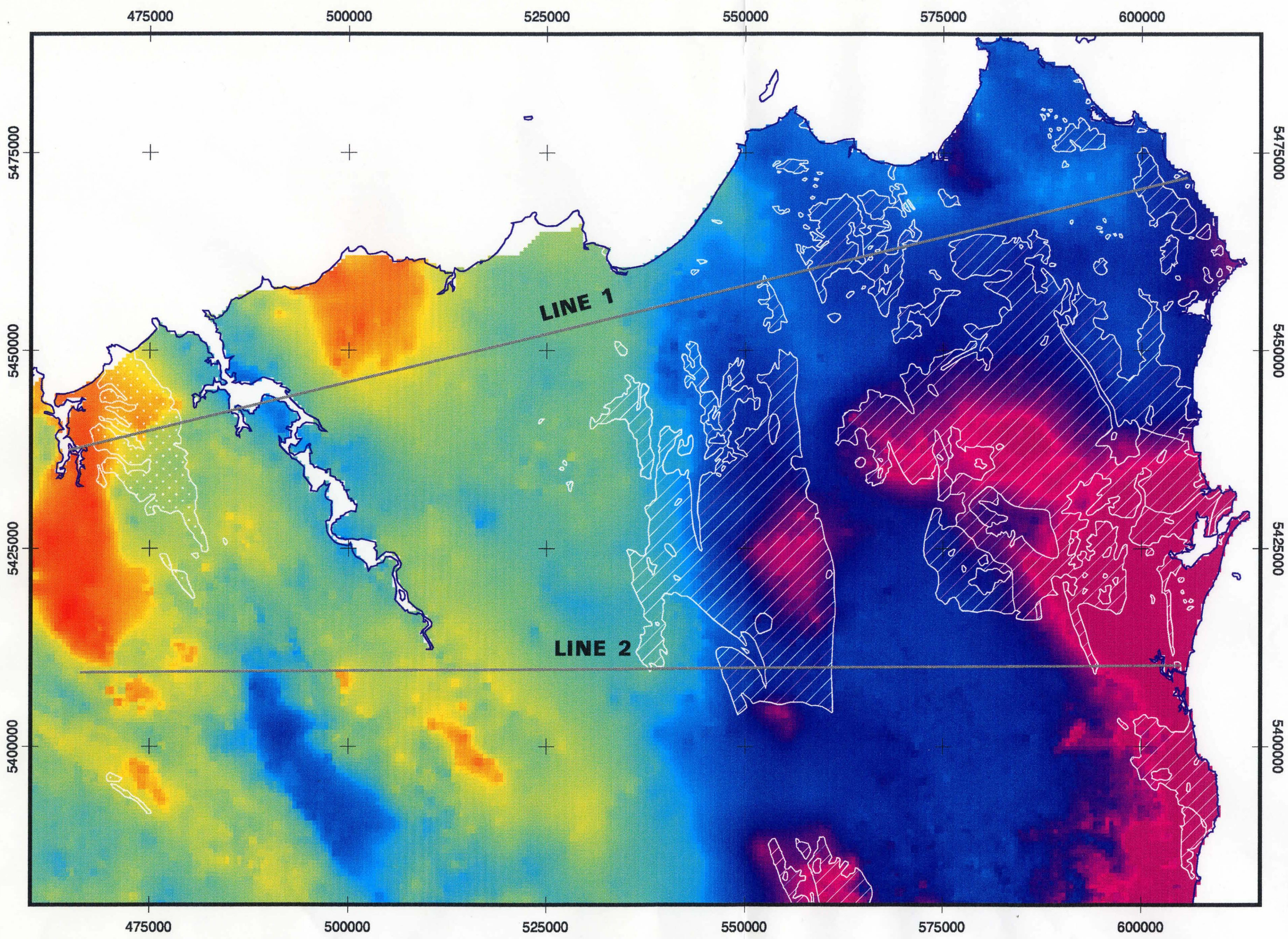


Figure 3

Gravity station distribution - northeast Tasmania





Hatched Area - Granitoids
 Stippled Area - Precambrian

Bouguer density 2.67 t/m³.
 MANTLE91 regional gravity model removed.
 Grid mesh size: 500 metres.

Geology from
 Mineral Resources Tasmania
 1:500,000 digital geology.

**NE TASMANIA
 RESIDUAL GRAVITY
 (MANTLE91)**

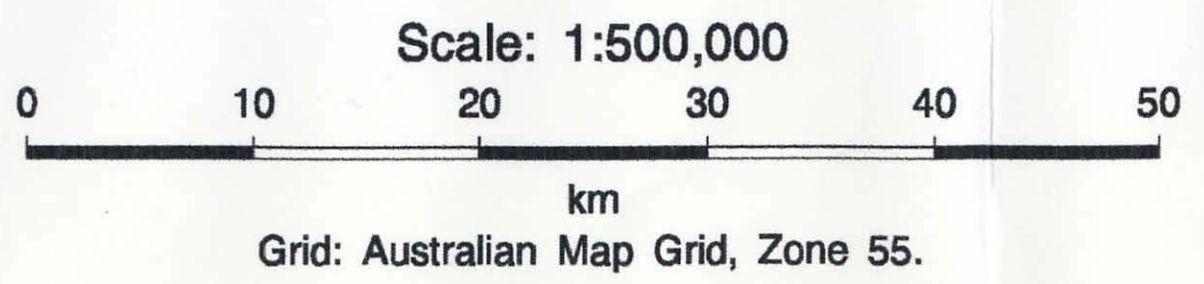
Figure 4

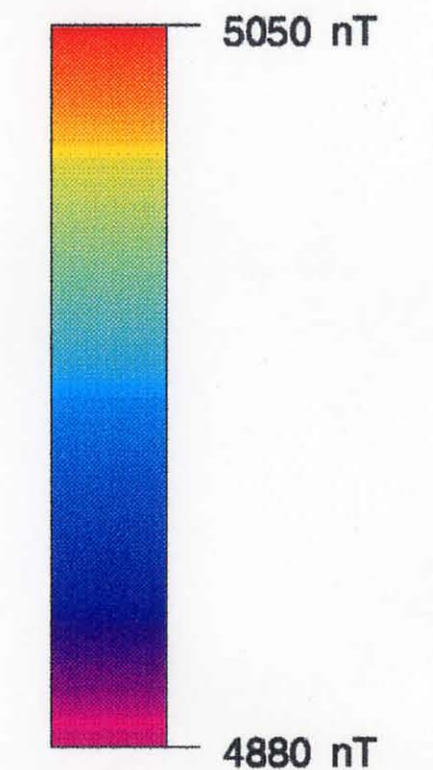
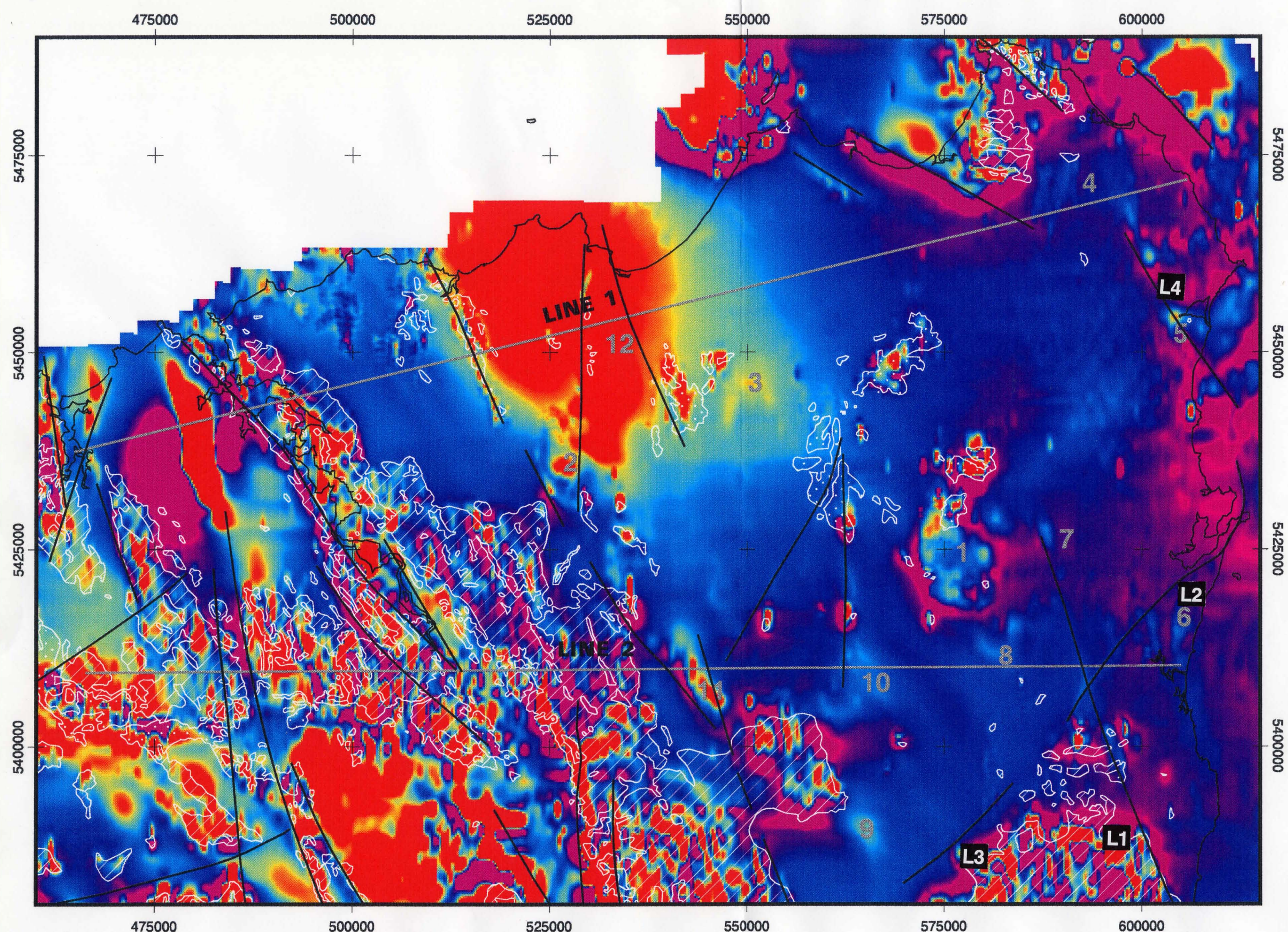
475000 500000 525000 550000 575000 600000

5475000
5450000
5425000
5400000

5475000
5450000
5425000
5400000

475000 500000 525000 550000 575000 600000

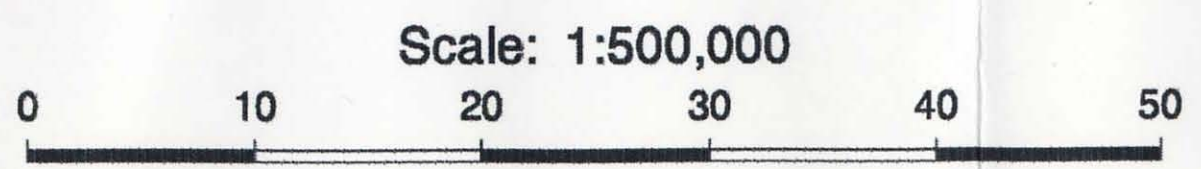




Hatched Area - Jurassic dolerite
 Stippled Area - Tertiary basalt

Digital data from AGSO regional survey, NETGOLD project and company surveys.
 Grid mesh size: 250 metres.

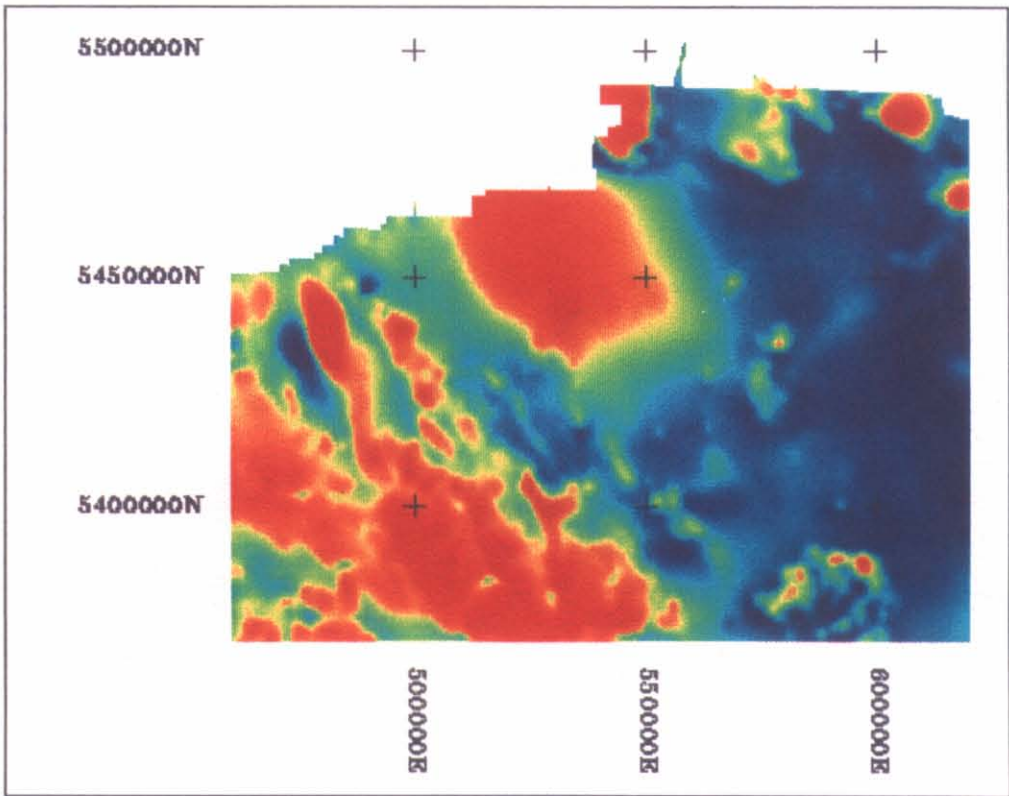
Geology from Mineral Resources Tasmania 1:500,000 digital geology.



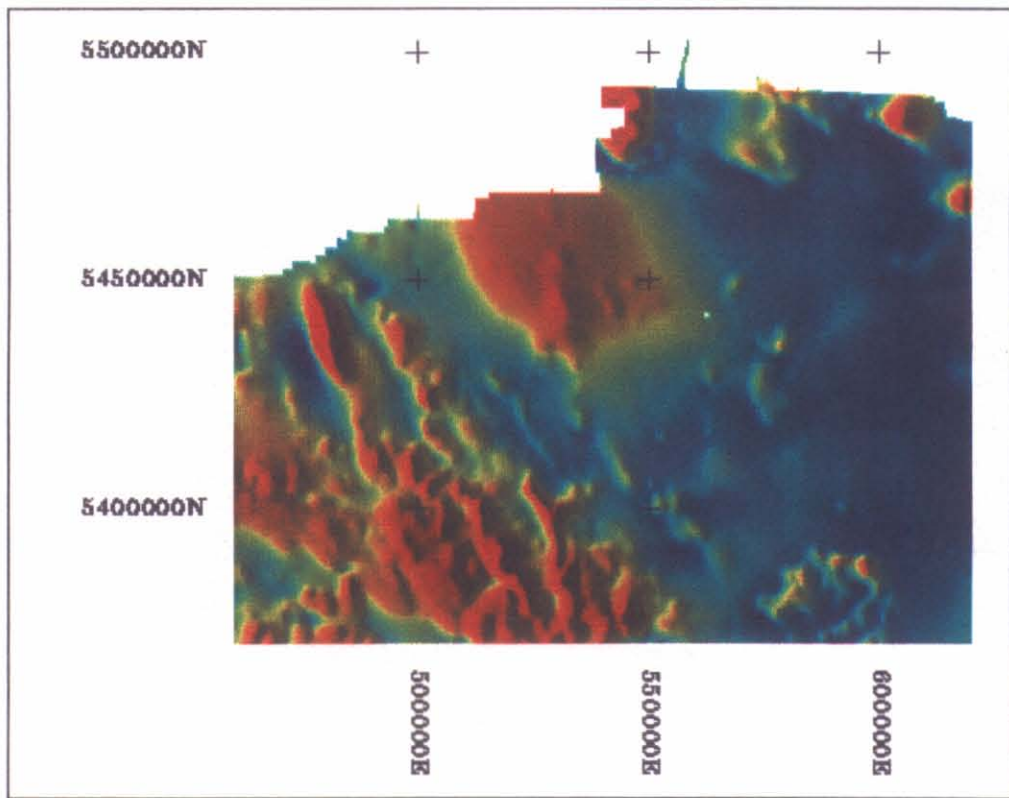
Scale: 1:500,000
 Grid: Australian Map Grid, Zone 55.

**NE TASMANIA
 TOTAL MAGNETIC
 INTENSITY**

Figure 5



(a) Pseudocolour



(b) Pseudocolour (Illumination from the west)

Figure 6

Aeromagnetic data upward continued 1500 m — northeast Tasmania

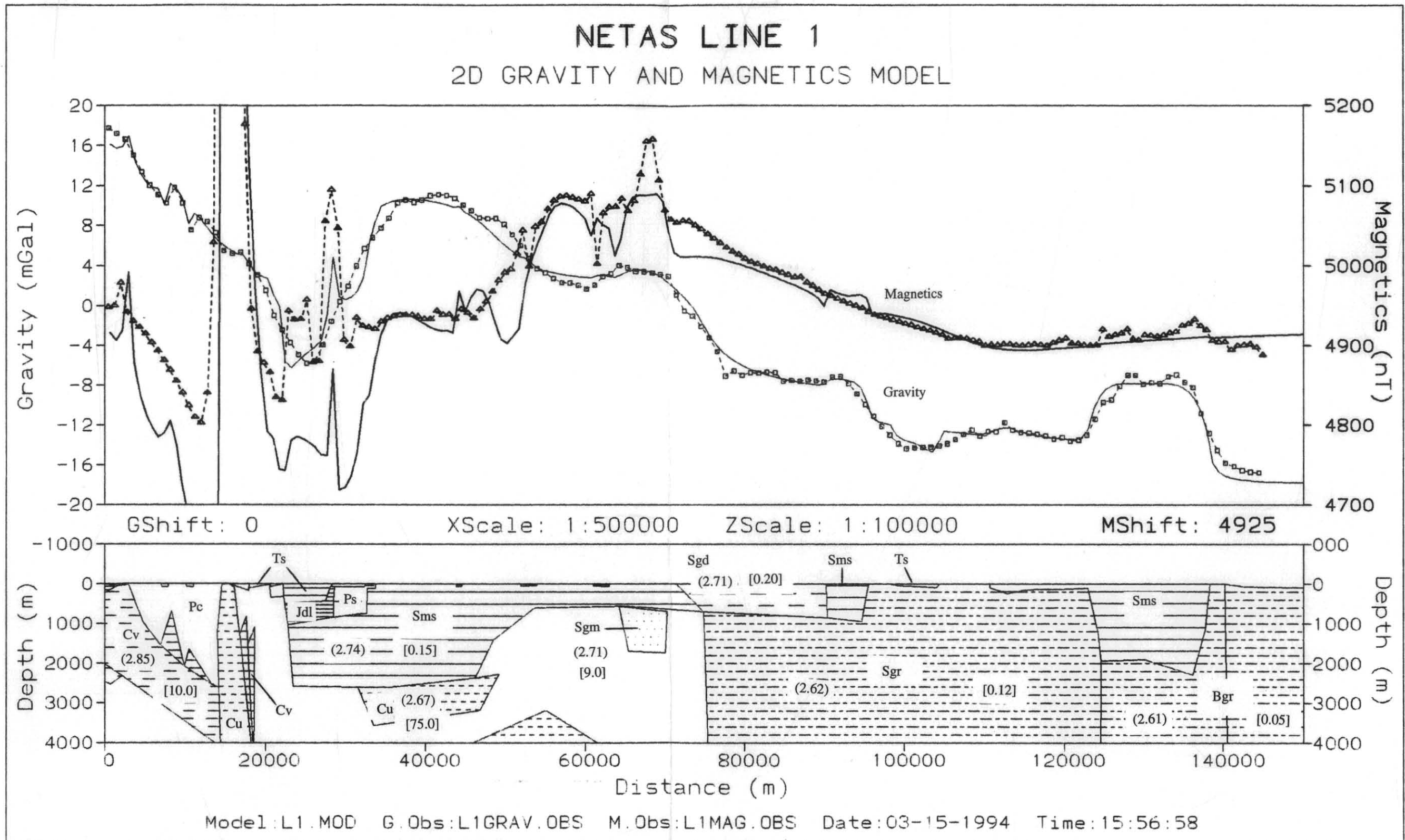
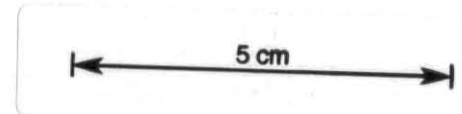


Figure 7

Two dimensional gravity and magnetic model from Port Sorell to Boulder Point.
 Values in curved brackets are densities (t/m^3);
 values in square brackets are magnetic susceptibilities [$\times 10^{-3}$ SI].



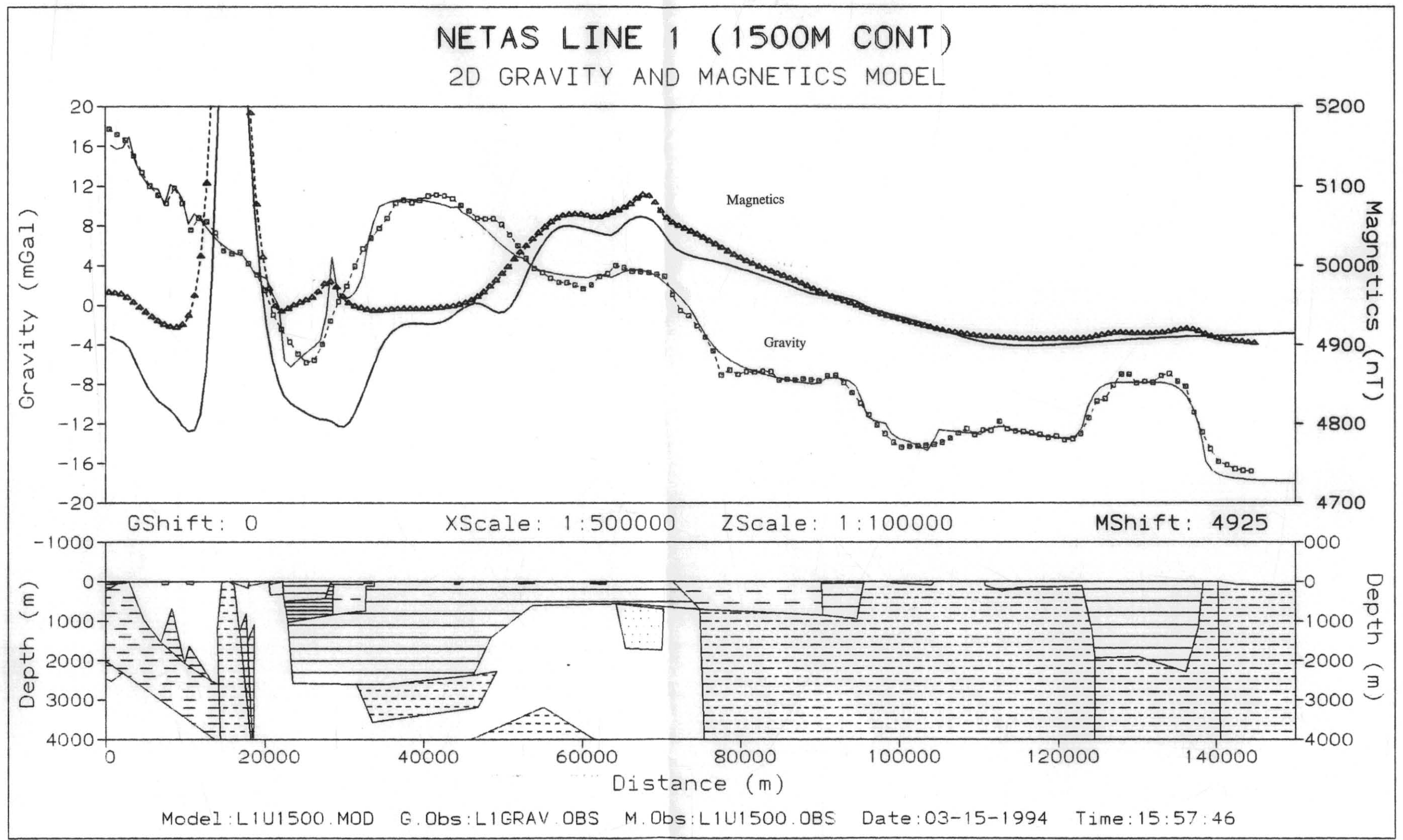
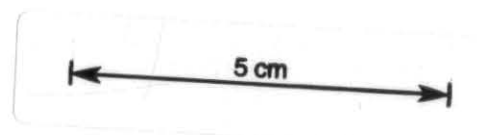


Figure 8

Two dimensional gravity and magnetic model from Port Sorell to Boulder Point with the aeromagnetic data upward continued 1500 m. Body parameters are shown on Figure 7.



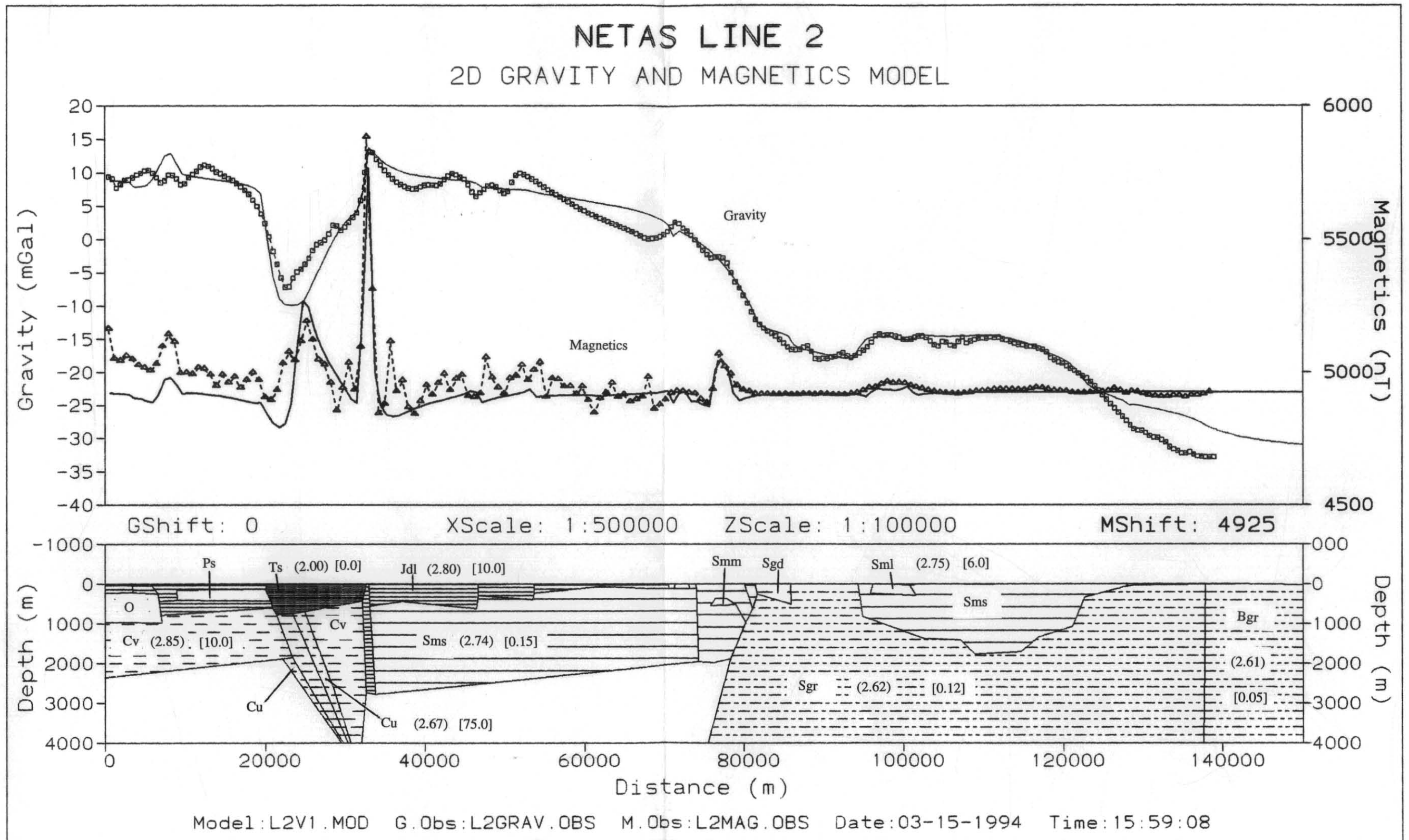
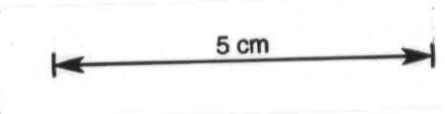


Figure 9

Two dimensional gravity and magnetic model from Elizabeth Town to Scamander.
 Values in curved brackets are densities (t/m^3);
 values in square brackets are magnetic susceptibilities [$\times 10^{-3}$ SI]



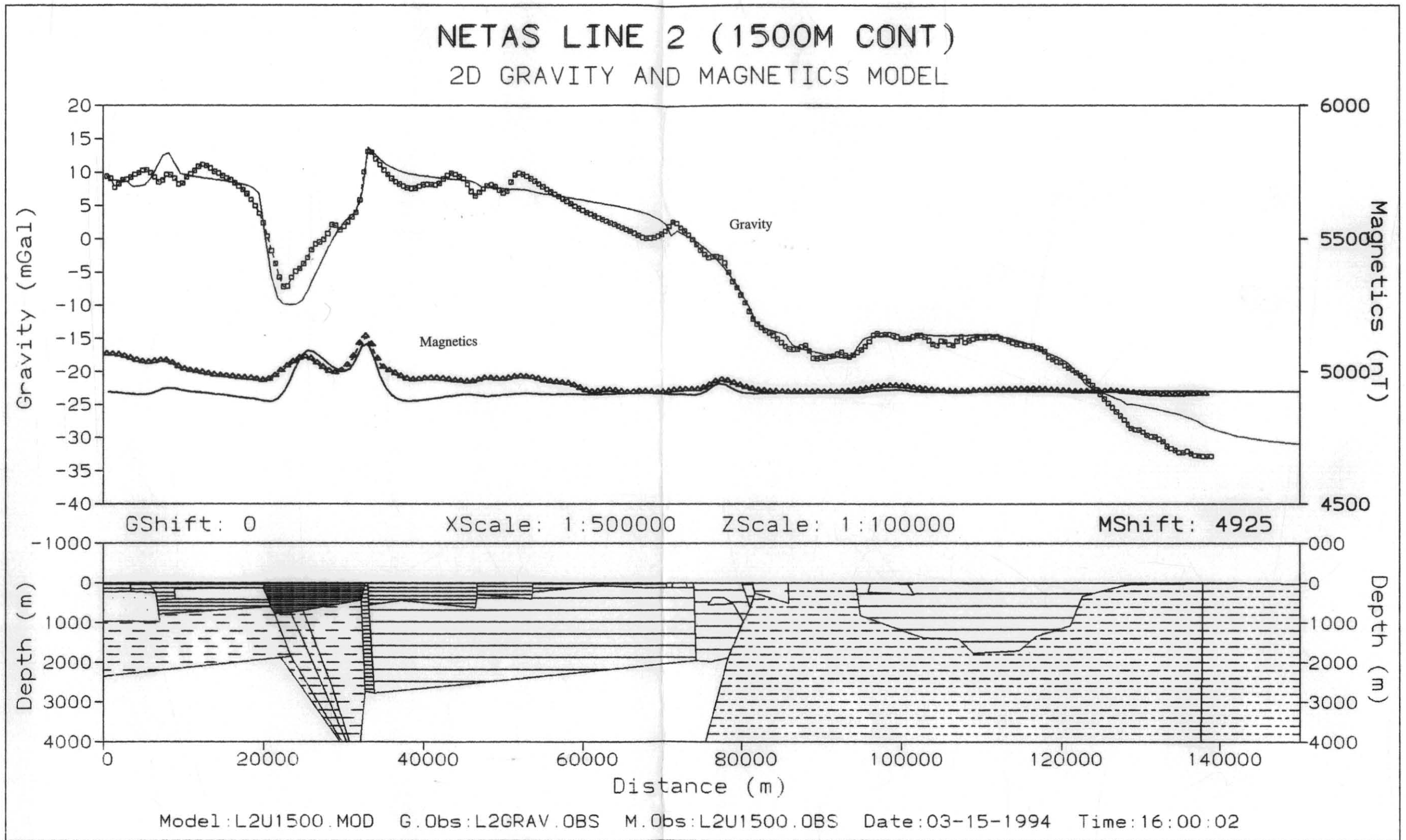


Figure 10

Two dimensional gravity and magnetic model from Elizabeth Town to Scamander with the aeromagnetic data upward continued 1500 m. Body parameters are shown on Figure 9.

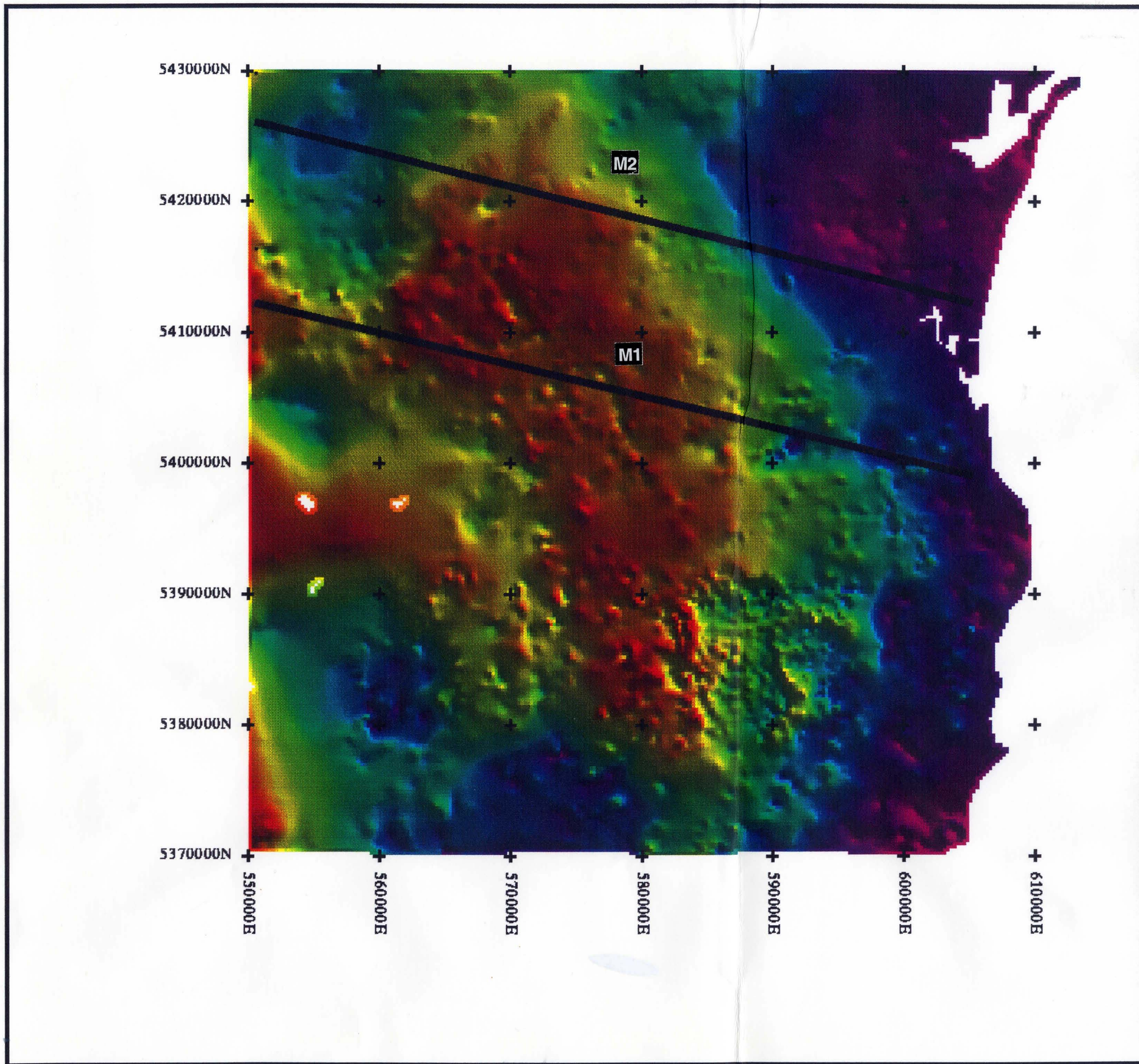


Figure 11
Residual gravity anomaly — Fingal NETGOLD area

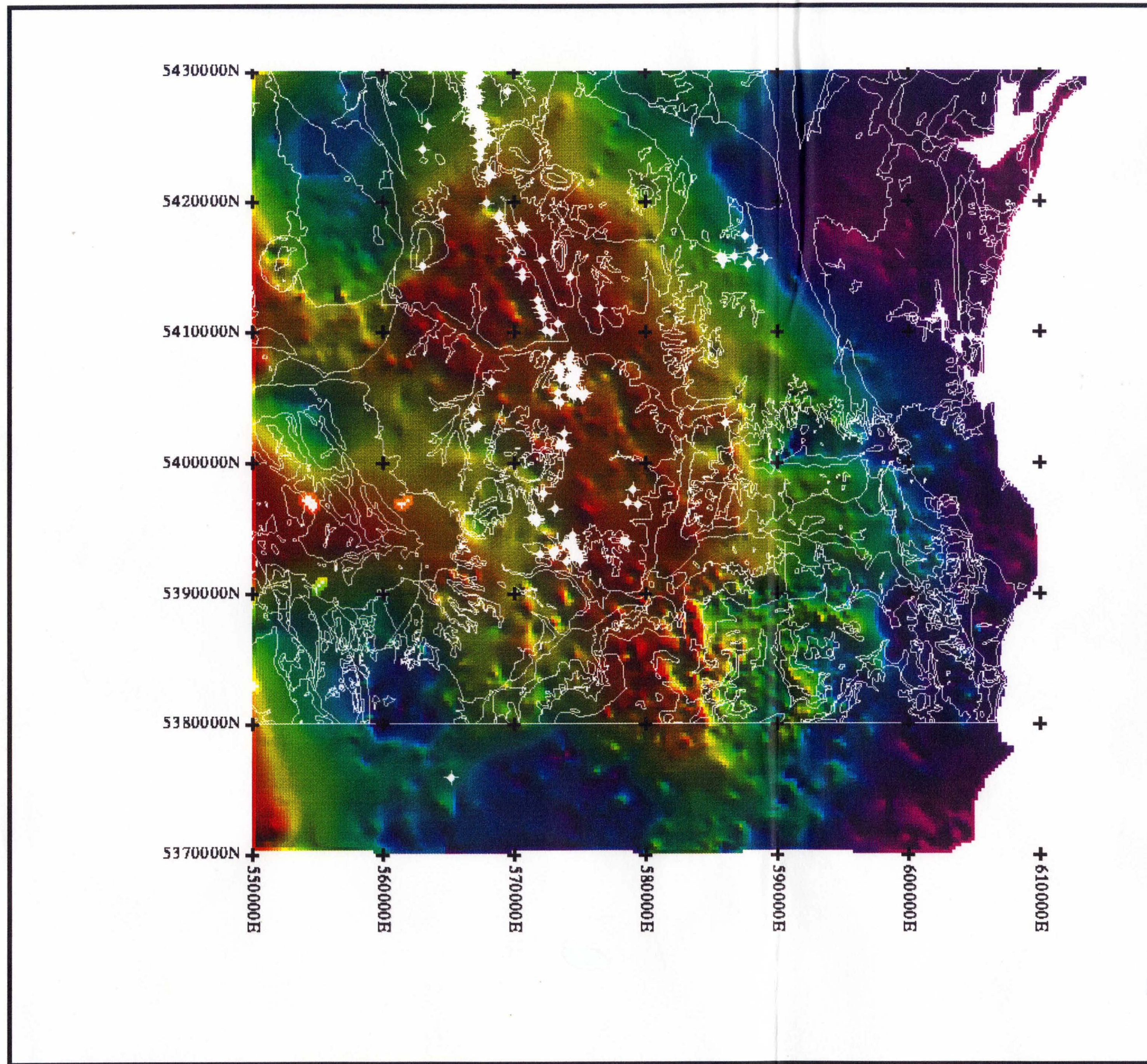


Figure 12

Residual gravity anomaly — Fingal NETGOLD area.
 Polygons from the 1:250 000 digital geology
 and primary gold mineralisation shown in white.

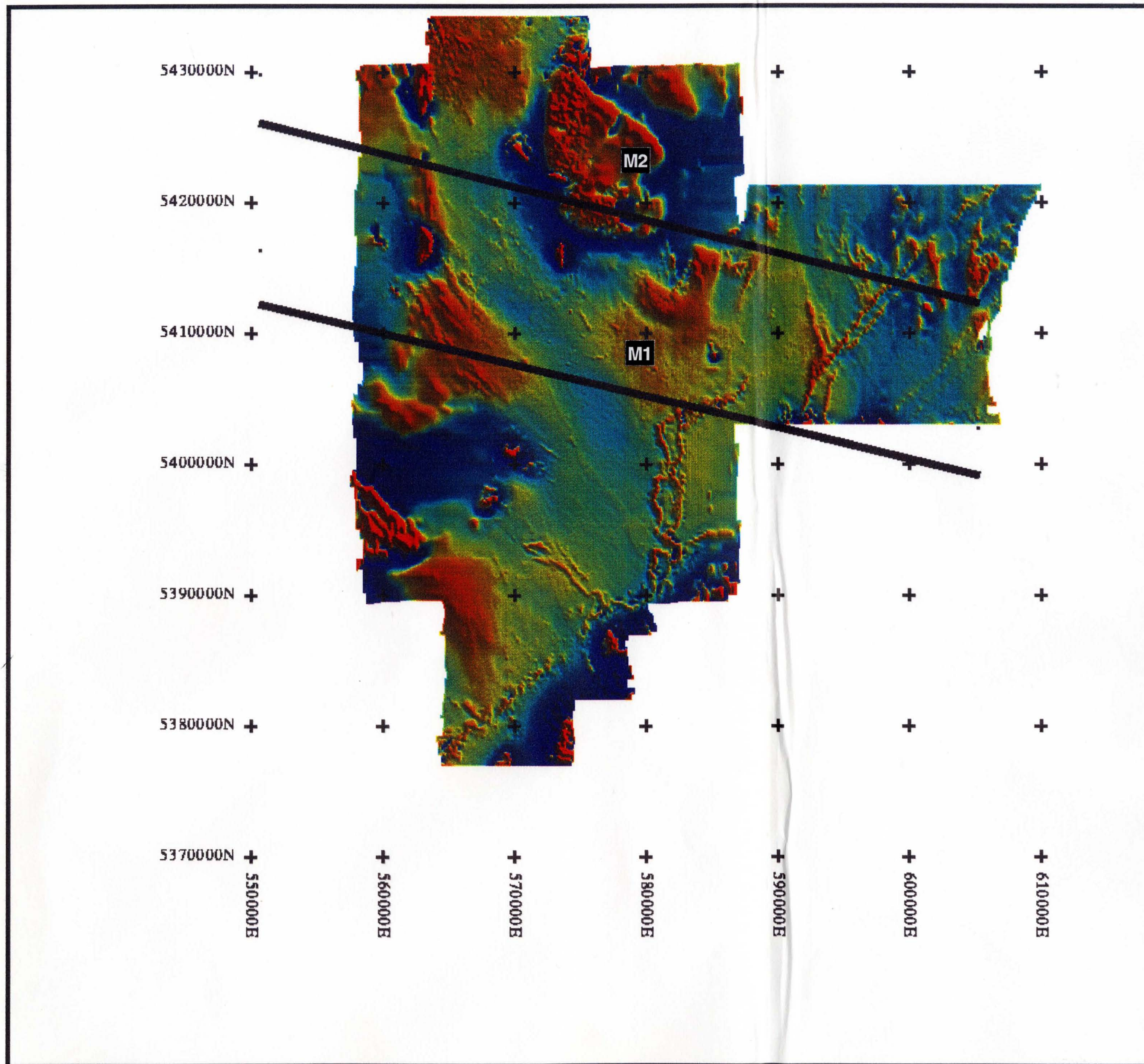


Figure 13
Residual magnetic intensity — Fingal NETGOLD area

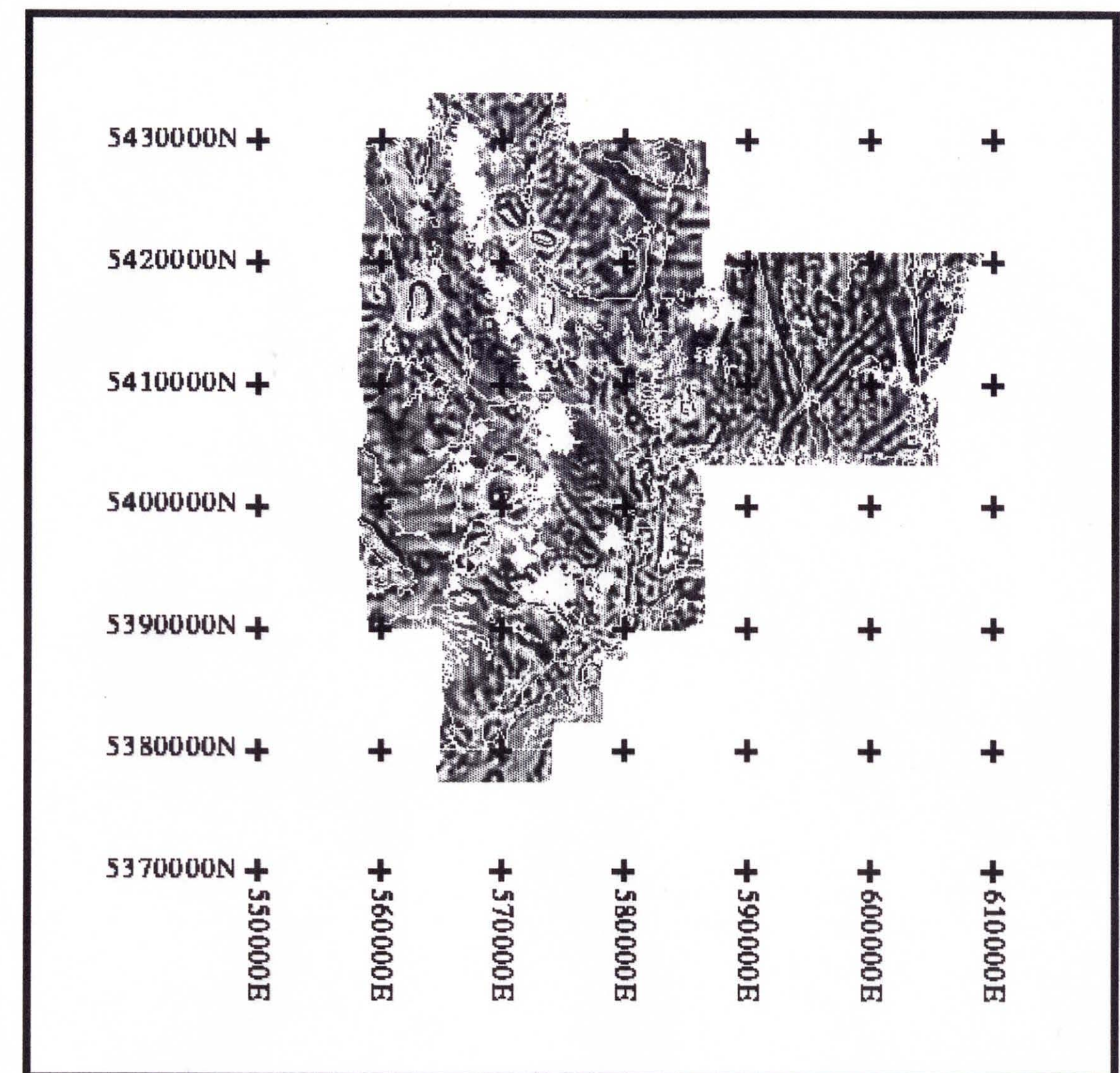
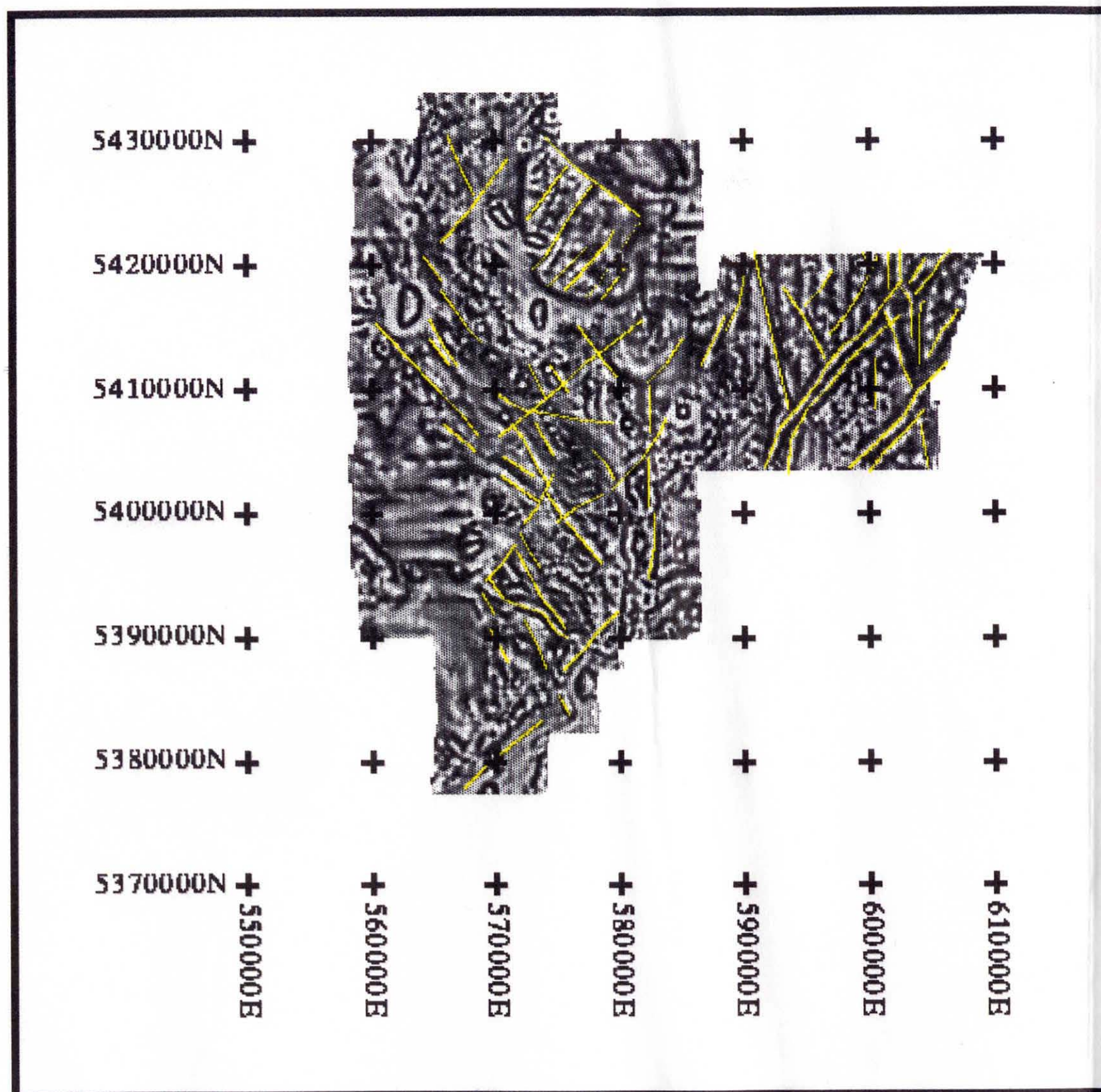


Figure 14

Automatic gain control filtered residual magnetic intensity — Fingal NETGOLD area

(a) Linear features shown in yellow

(b) Polygons from the 1:250 000 digital geology and primary gold mineralisation shown in white

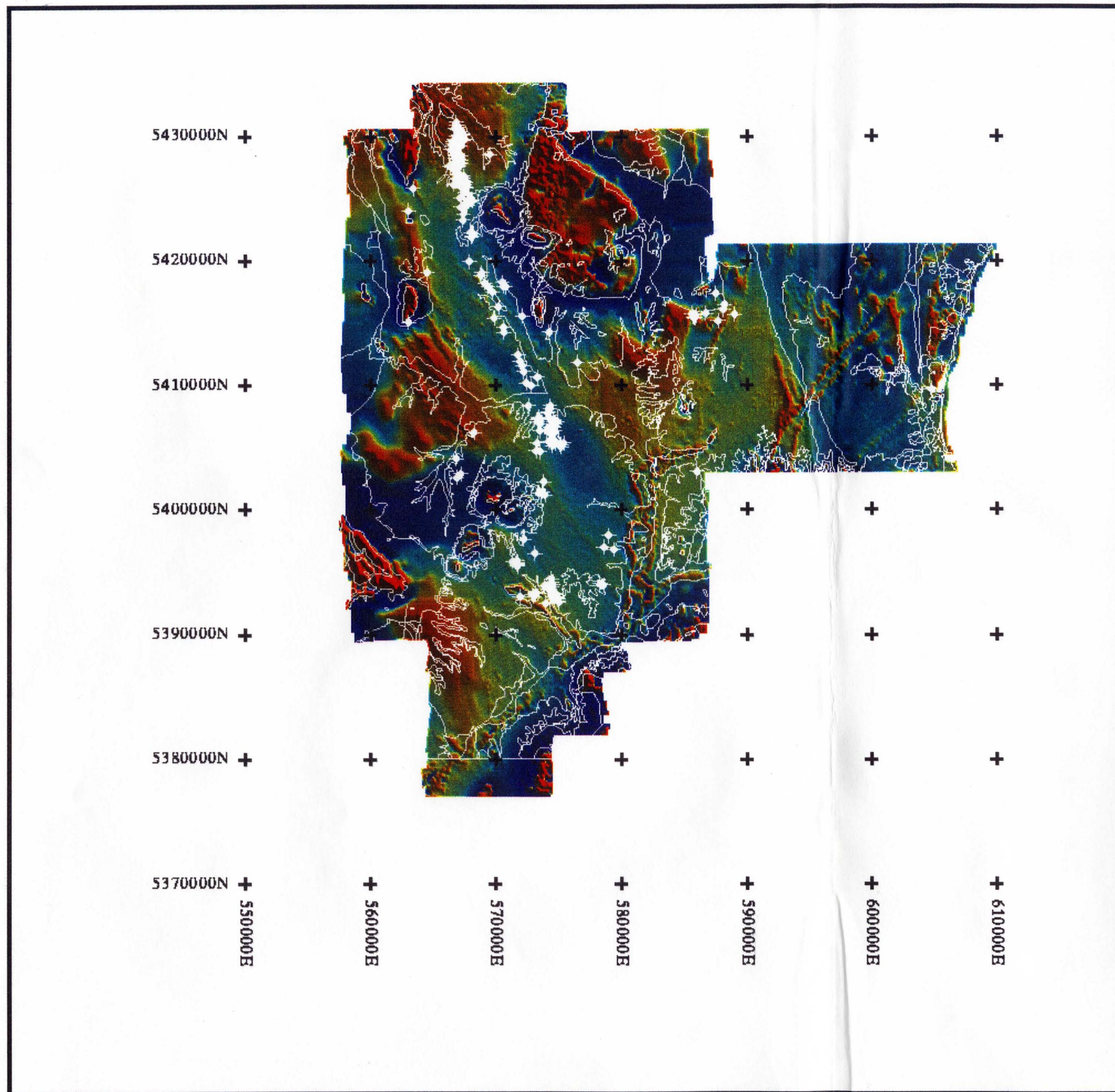


Figure 15

Residual magnetic intensity — Fingal NETGOLD area.
 Polygons from the 1:250 000 digital geology and
 primary gold mineralisation shown in white.

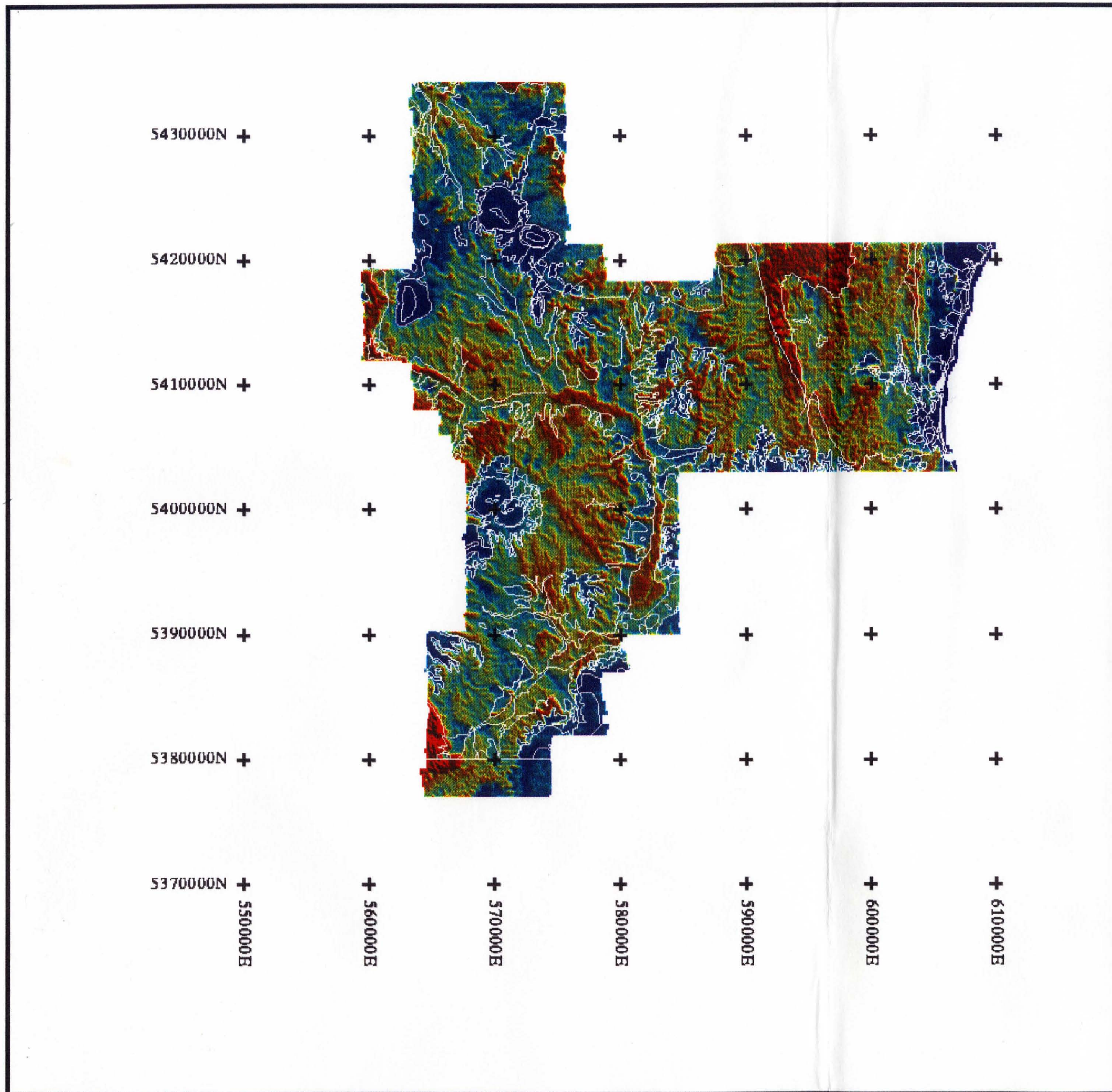


Figure 16
 Radiometric total counts — Fingal NETGOLD area.
 Polygons from the 1:250 000 digital geology shown in white.

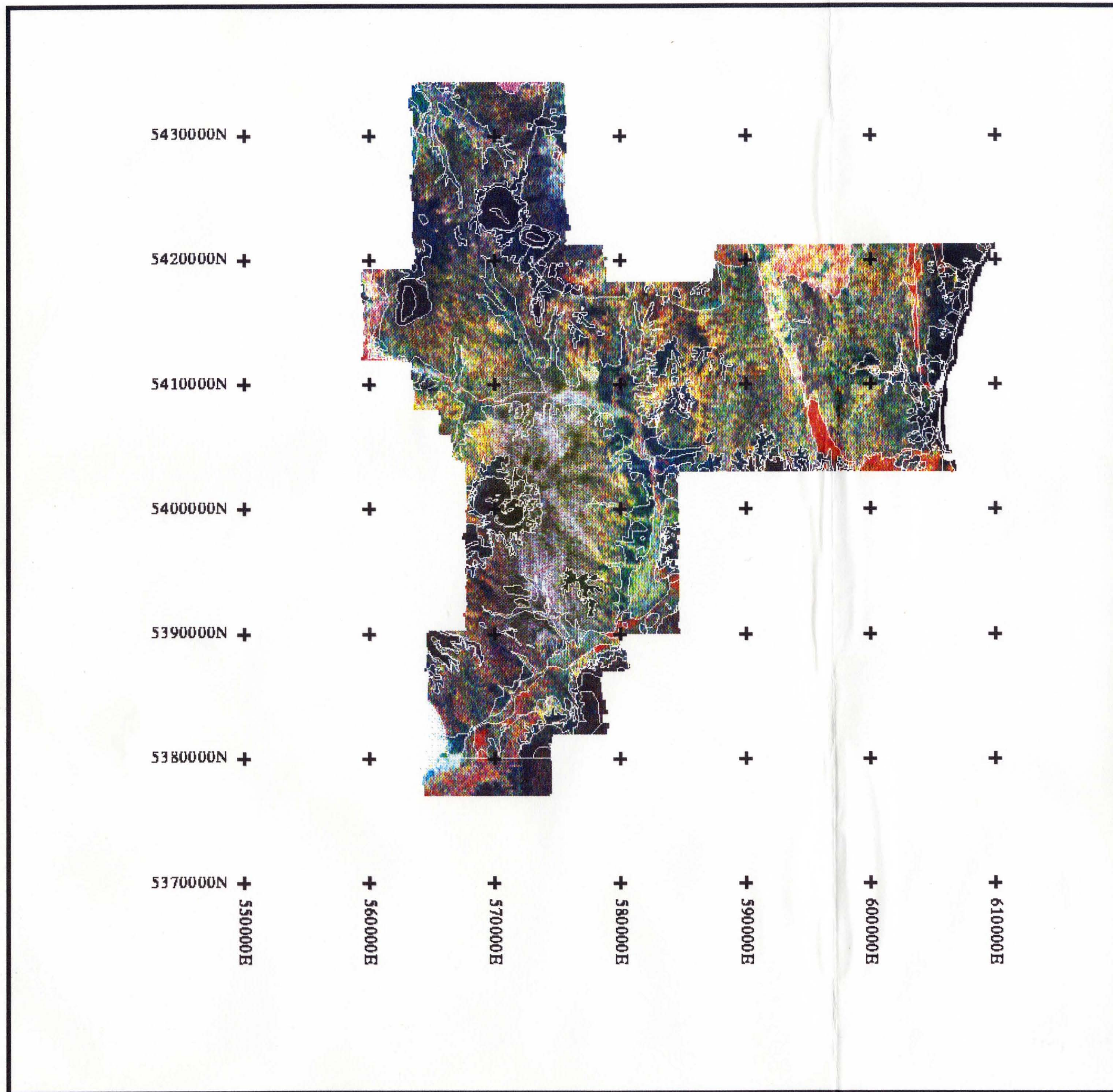


Figure 17

Radiometric element colour composite — Fingal NETGOLD area.
 Polygons from the 1:250 000 digital geology shown in white.
 (K=Red, Th=Green, U=Blue).

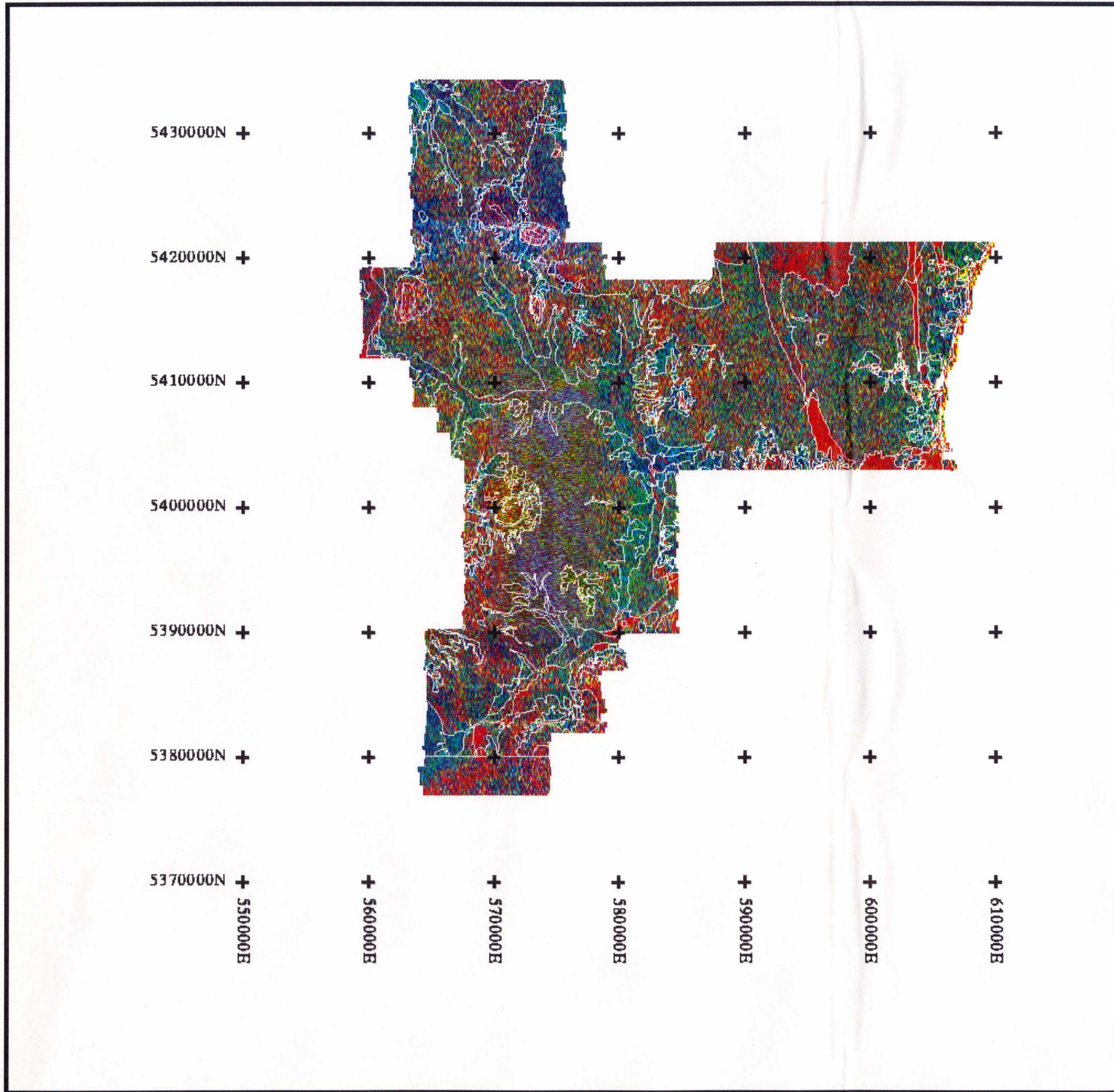


Figure 18

Radiometric ratio colour composite — Fingal NETGOLD area.
 Polygons from the 1:250 000 digital geology shown in white
 (K/TC=Red, Th/TC=Green, U/TC=Blue)

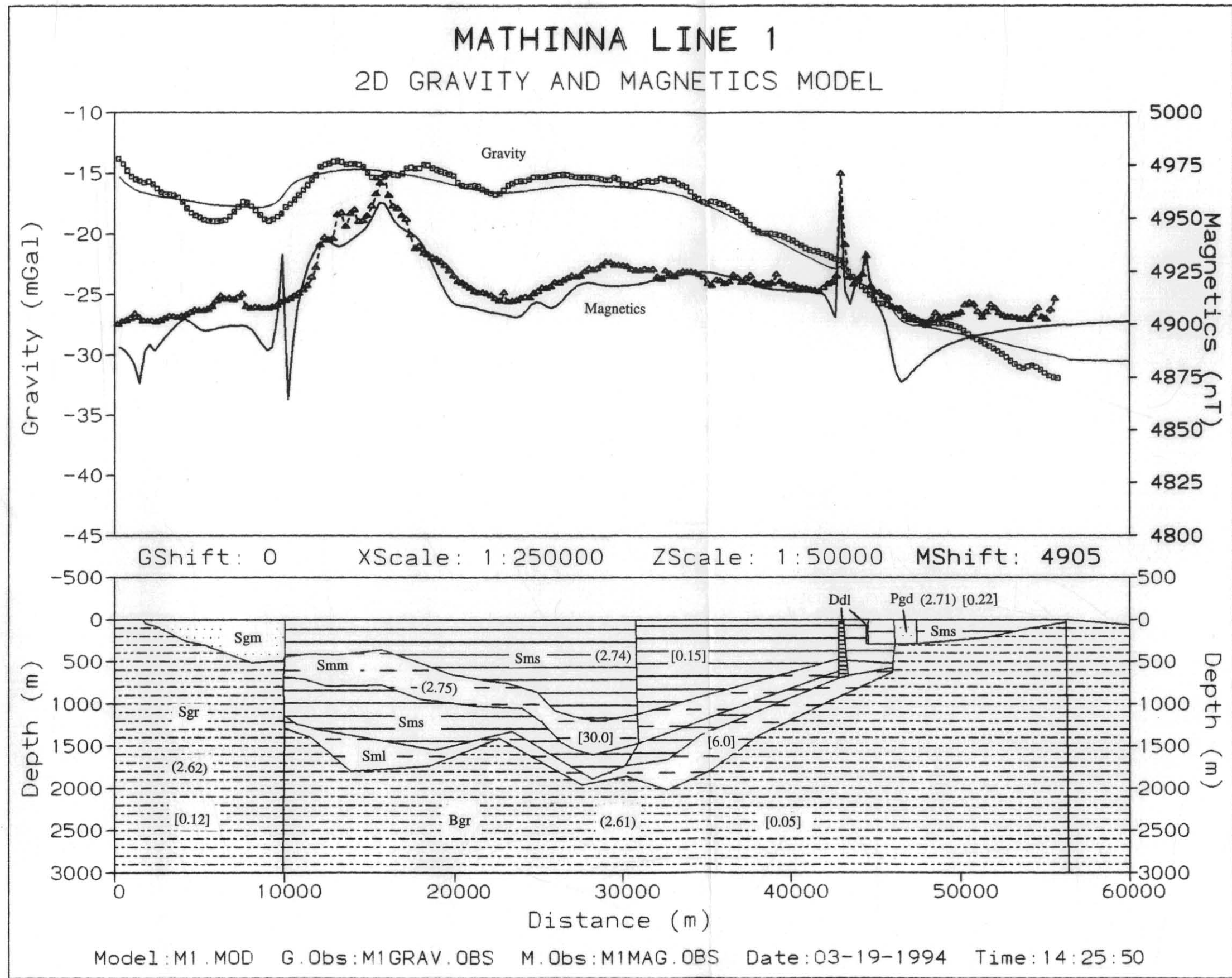
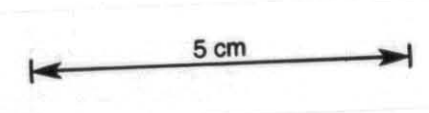


Figure 19

Two dimensional gravity and magnetic model of the Mathinna area. Values in curved brackets are densities (t/m^3); values in square brackets are magnetic susceptibilities [$\times 10^{-3}$ SI].



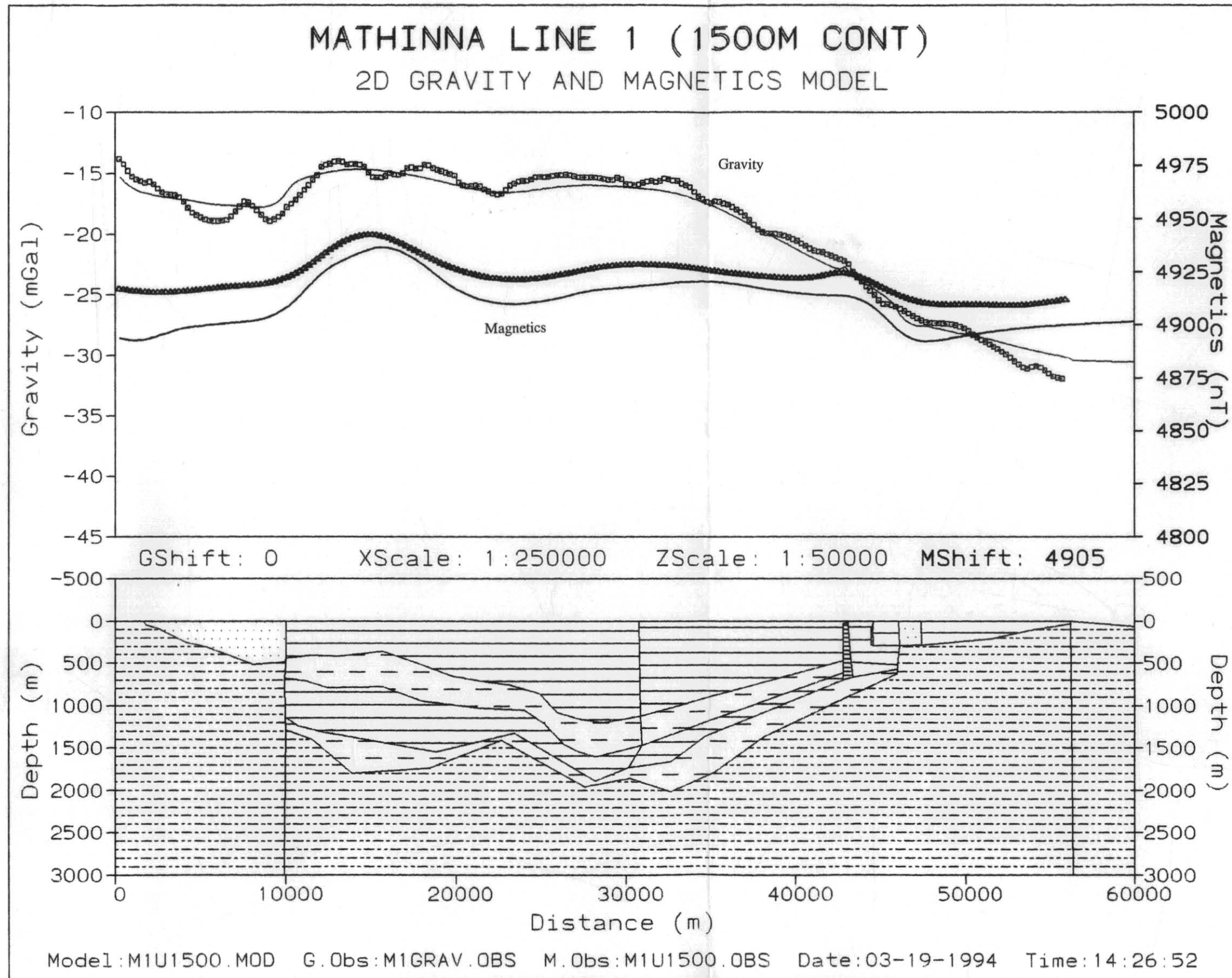
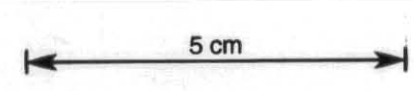


Figure 20

Two dimensional gravity and magnetic model of the Mathinna area with the magnetic data upward continued 1500 m. Body parameters are shown on Figure 19.



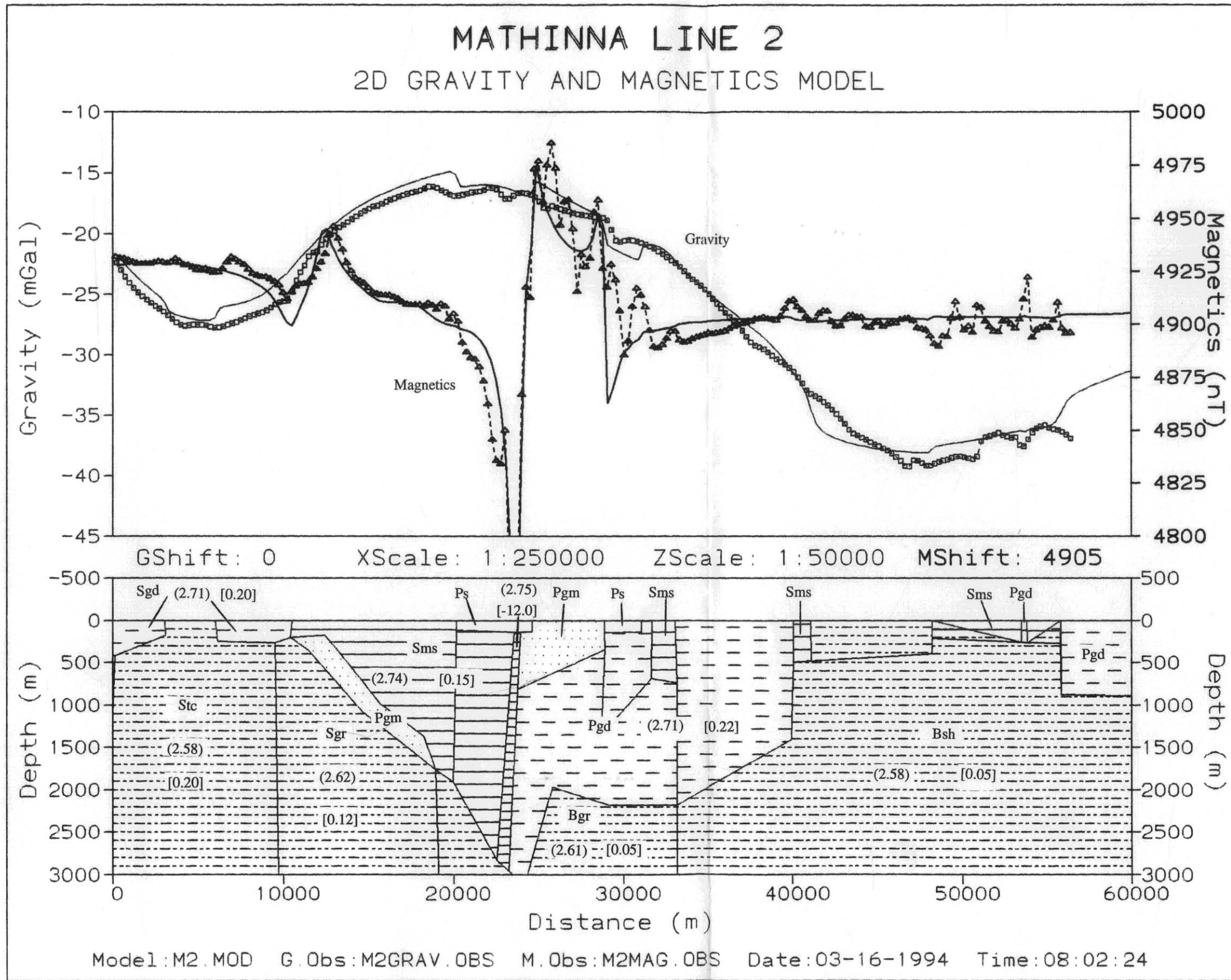
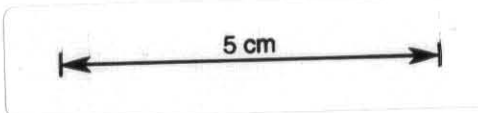


Figure 21

Two dimensional gravity and magnetic model of the Mt Victoria area. Values in curved brackets are densities (t/m^3); values in square brackets are magnetic susceptibilities [$\times 10^{-3}$ SI].



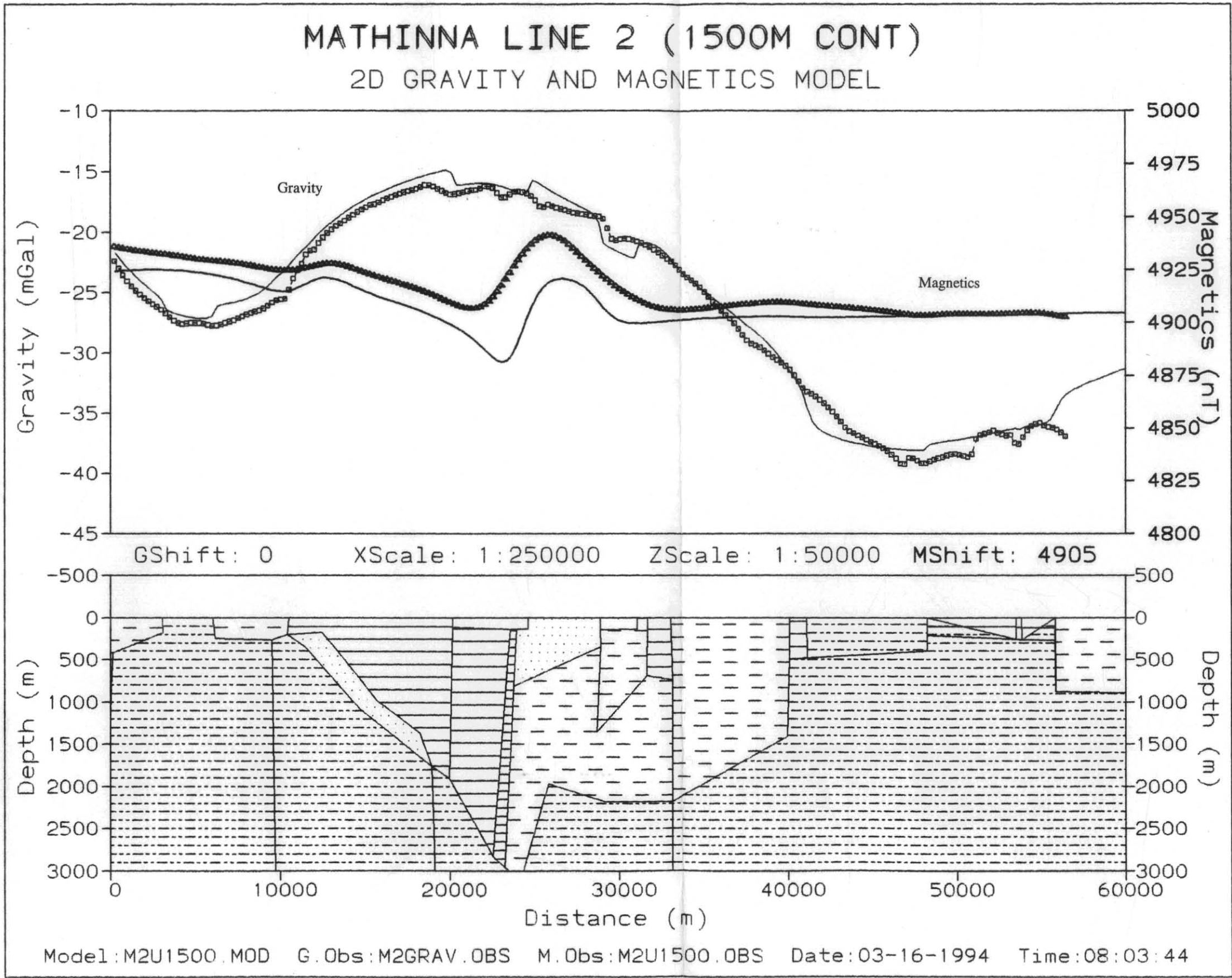
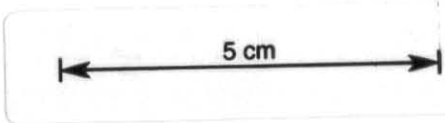


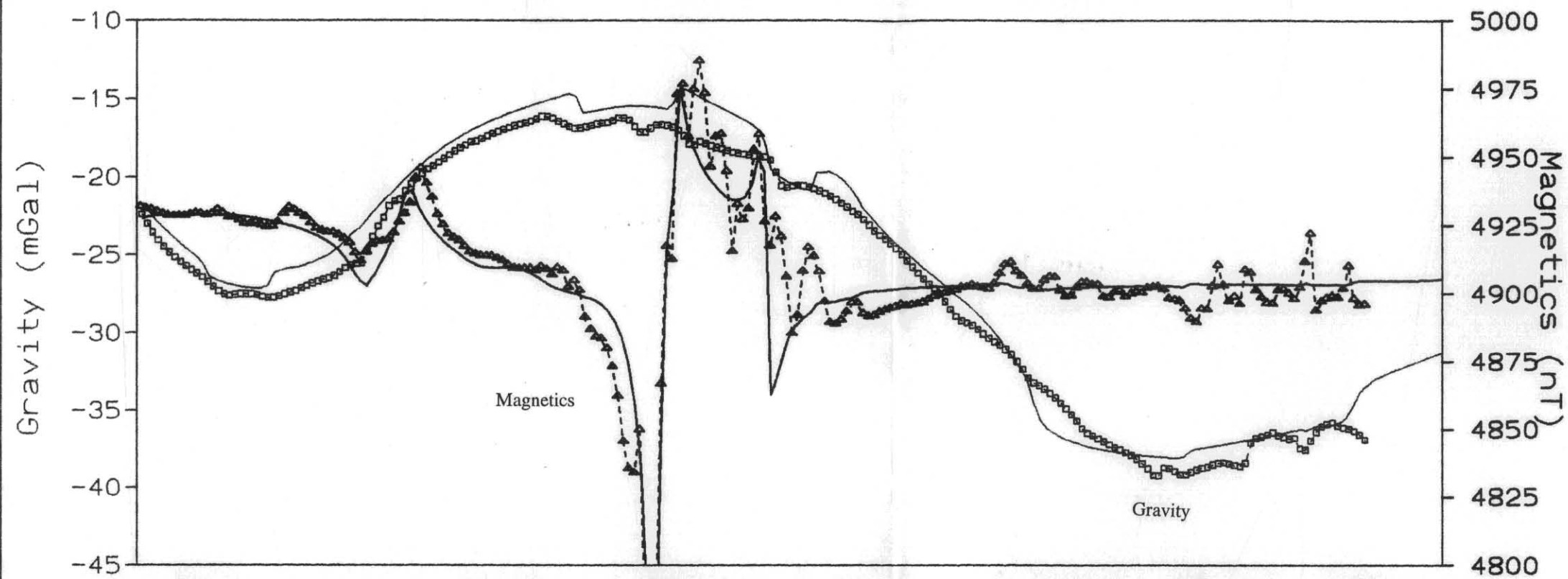
Figure 22

Two dimensional gravity and magnetic model of the Mt Victoria area with the magnetic data upward continued 1500 m. Body parameters are shown on Figure 21.

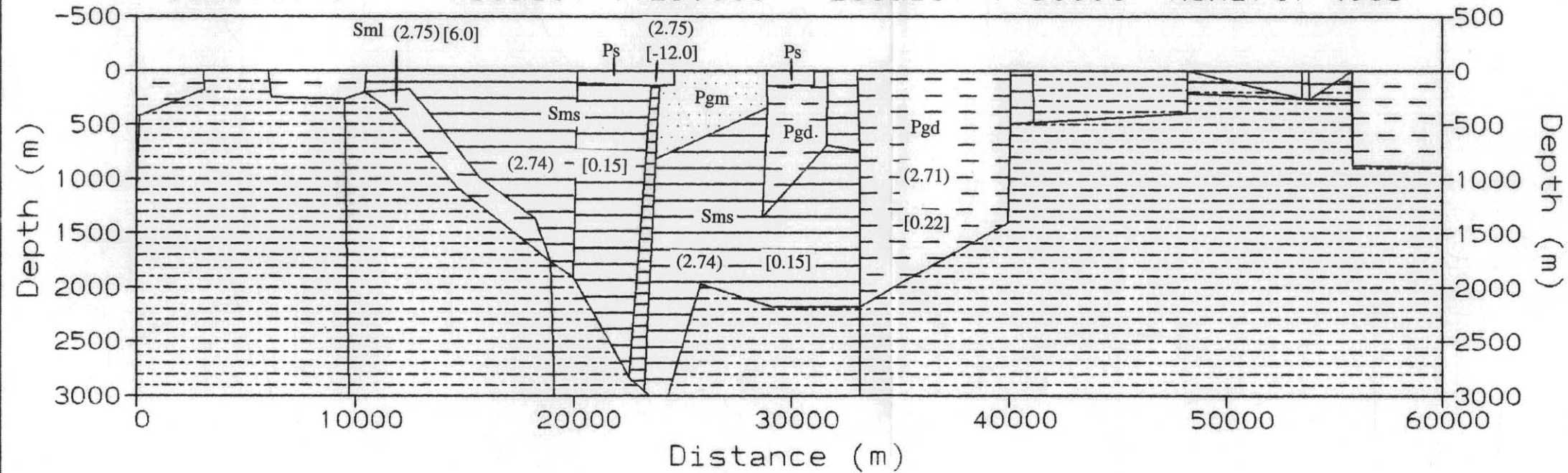


MATHINNA LINE 2 (MAGNETIC MATHINNA GROUP)

2D GRAVITY AND MAGNETICS MODEL



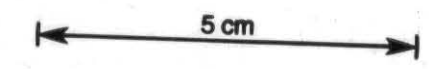
GShift: 0 XScale: 1:250000 ZScale: 1:50000 MShift: 4905



Model: M2MATHIN.MOD G.Obs: M2GRAV.OBS M.Obs: M2MAG.OBS Date: 03-16-1994 Time: 08:03:04

Figure 23

Two dimensional gravity and magnetic model of the Mt Victoria area with Mathinna Group rocks replacing concealed granodiorite. Values in curved brackets are densities (t/m³); values in square brackets are magnetic susceptibilities [x 10⁻³ SI]. Body parameters not shown on this figure are shown on Figure 21.



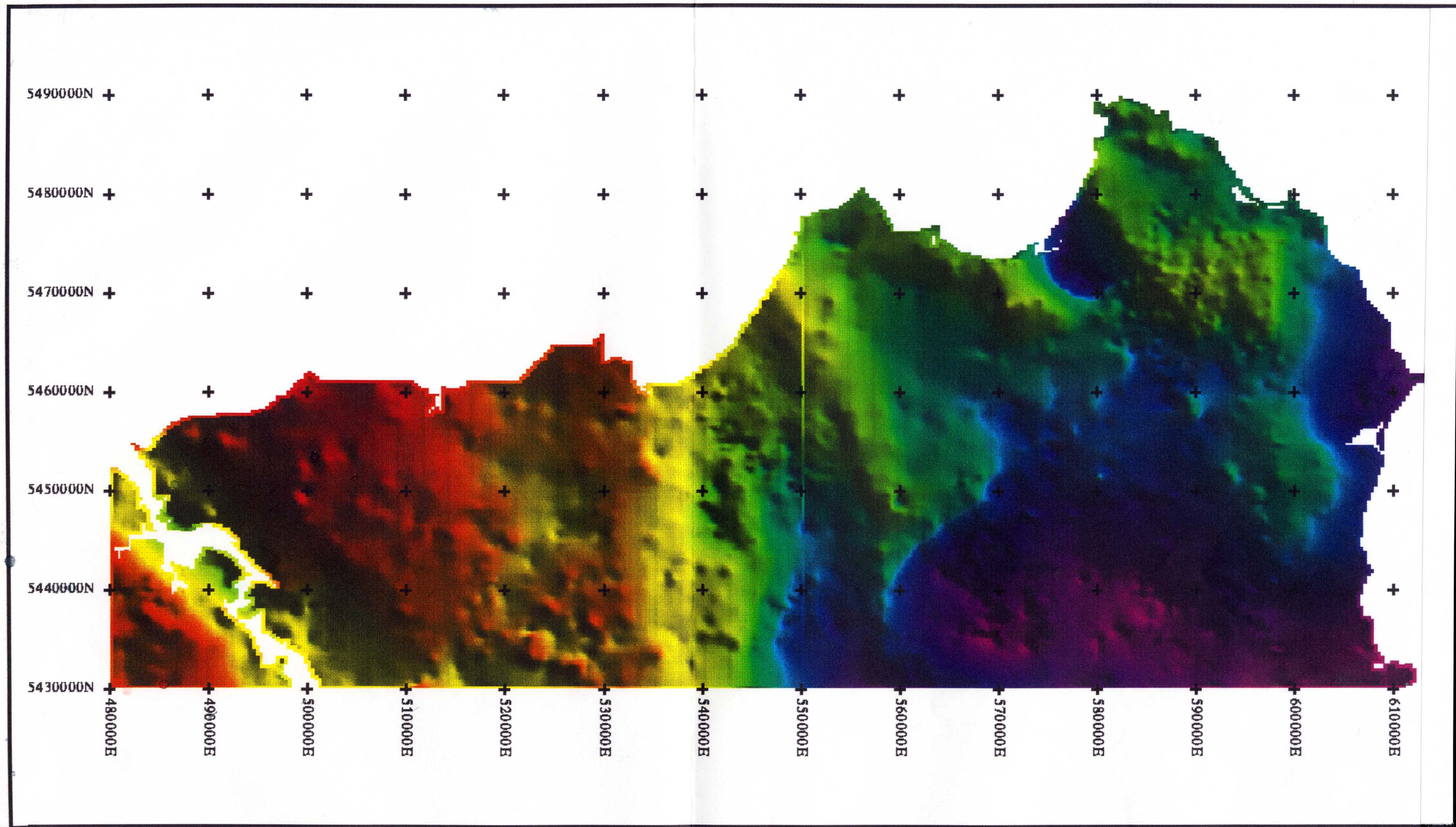


Figure 24
Residual gravity anomaly — NETGOLD northern coastal area

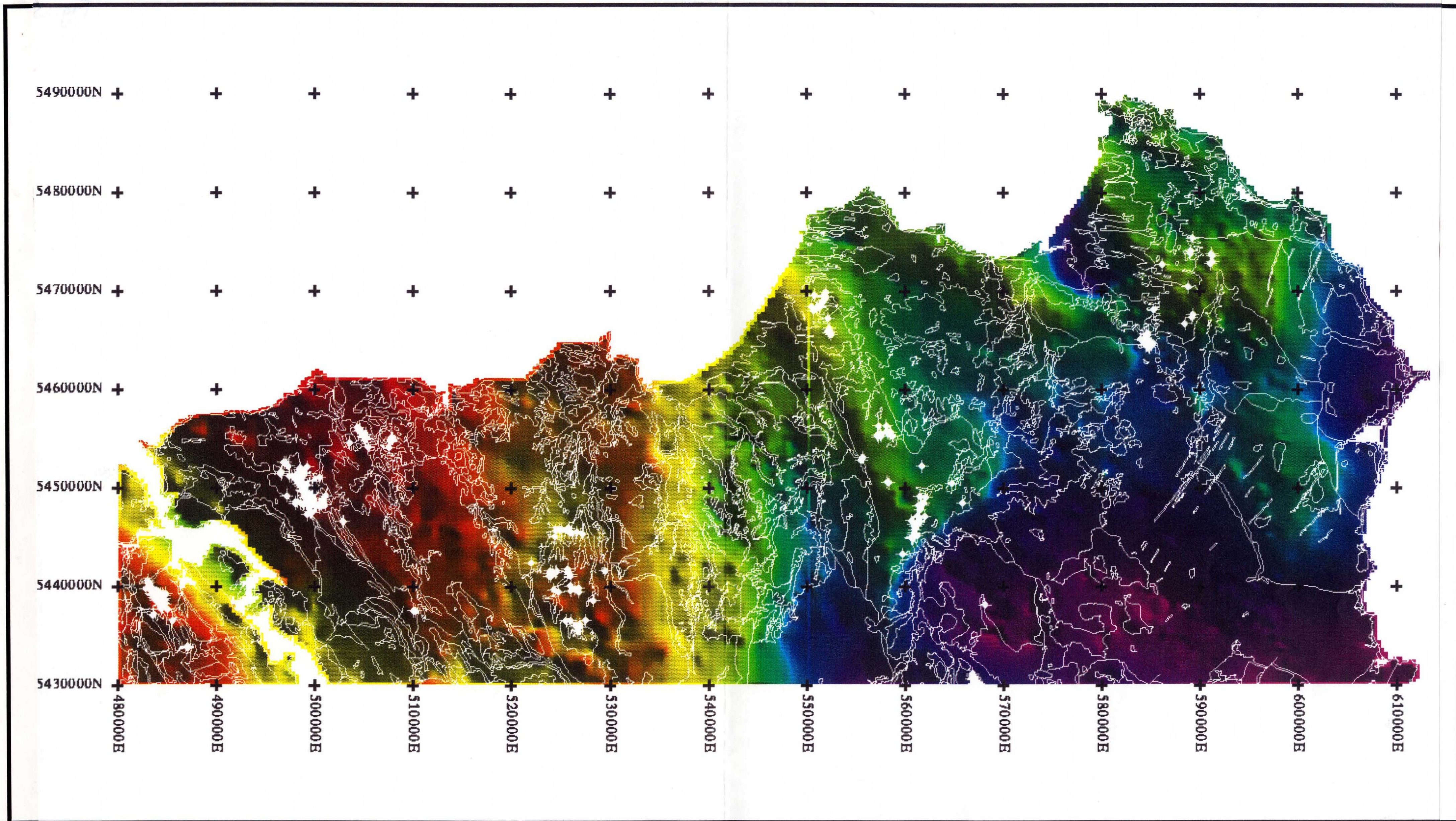


Figure 25

Residual gravity anomaly — NETGOLD northern coastal area.
 Polygons from the 1:250 000 digital geology and primary gold mineralisation shown in white.

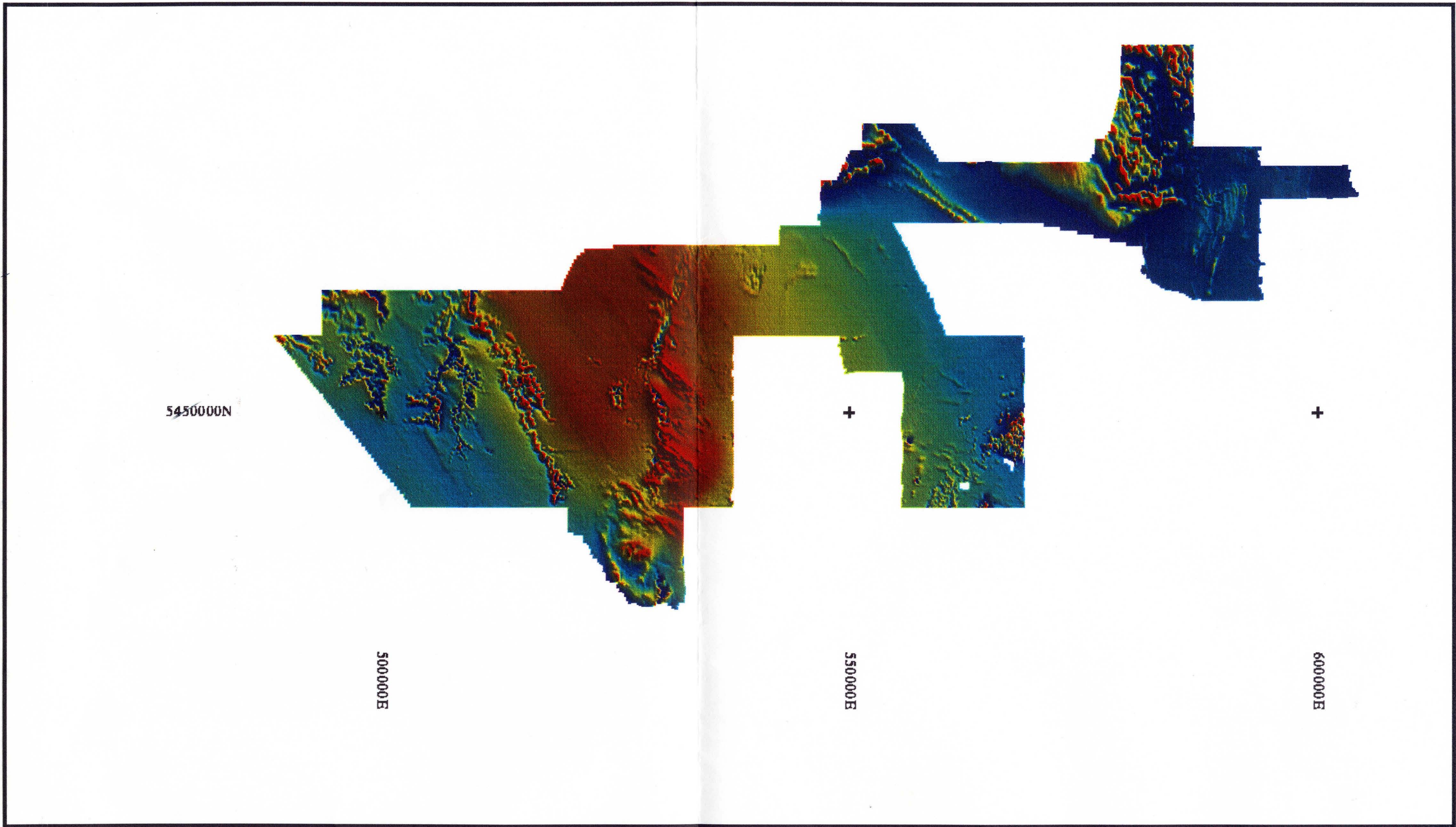


Figure 26
Residual magnetic intensity — NETGOLD northern coastal area



Figure 27

Automatic gain control filtered residual magnetic intensity — NETGOLD northern coastal area.
Linear features shown in yellow.

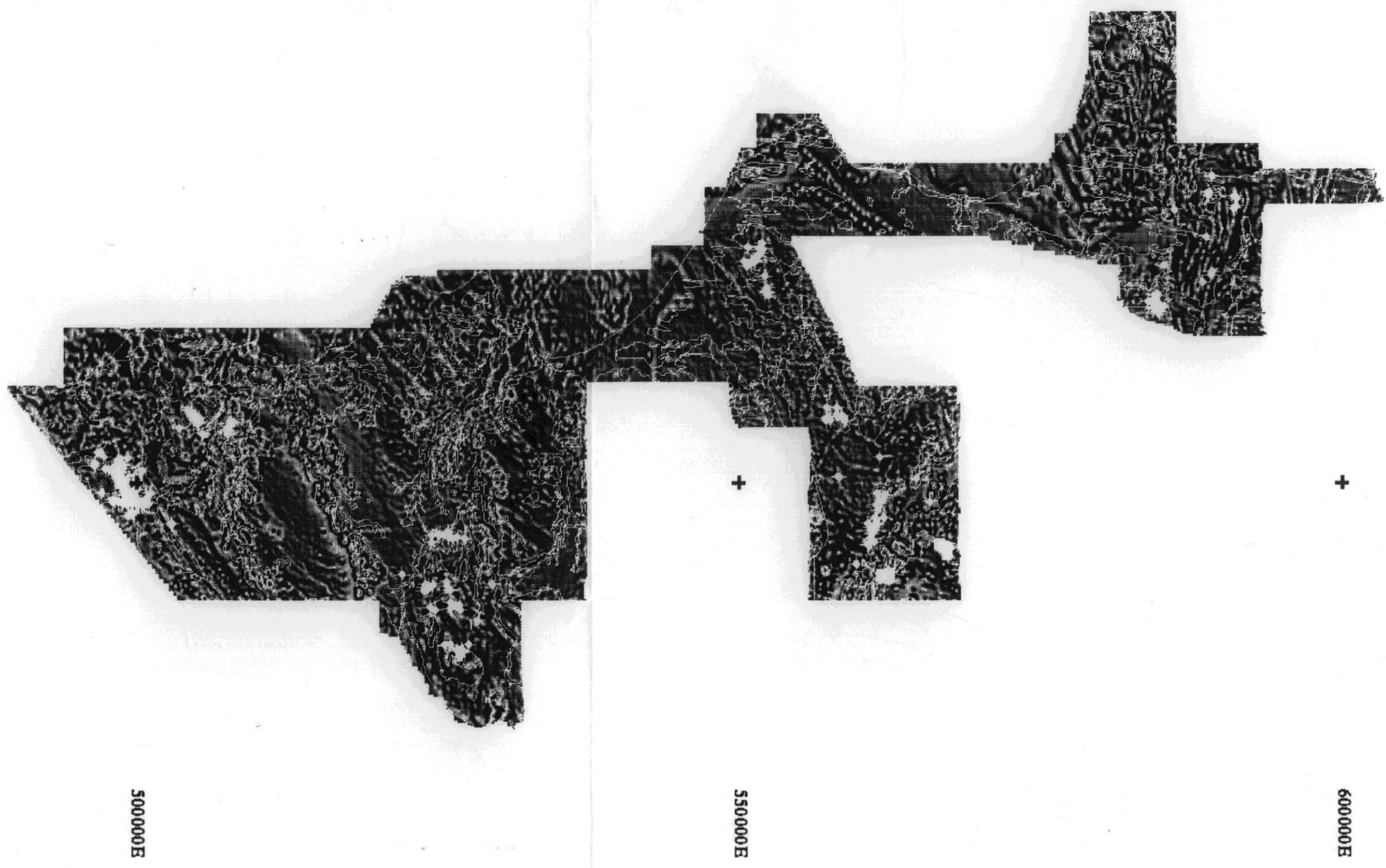
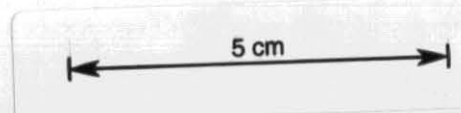


Figure 28

Automatic gain control filtered residual magnetic intensity — NETGOLD northern coastal area.
Polygons from the 1:250 000 digital geology and primary gold mineralisation shown in white.



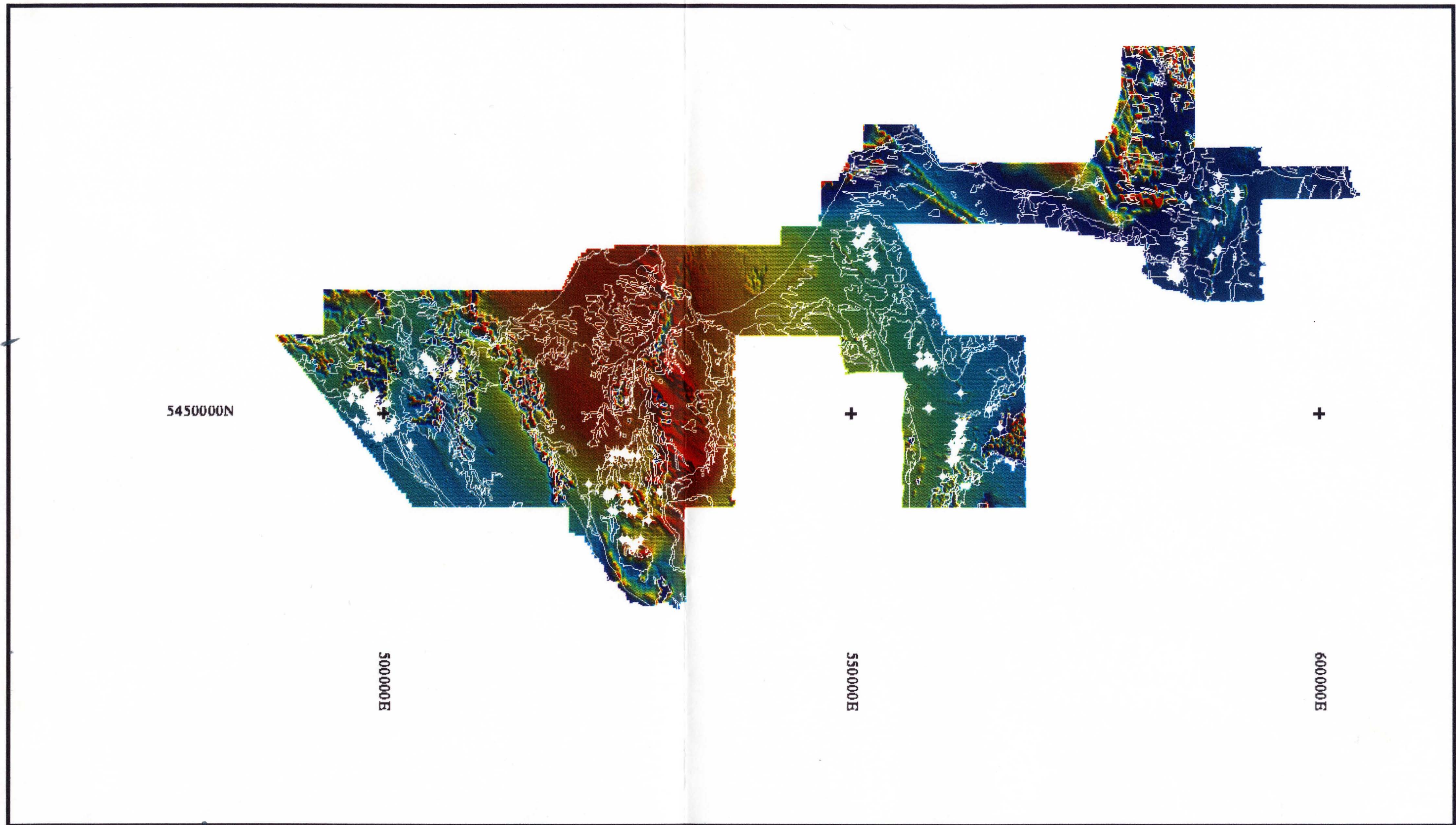


Figure 29

Residual magnetic intensity — NETGOLD northern coastal area.
 Polygons from the 1:250 000 digital geology and primary gold mineralisation shown in white.

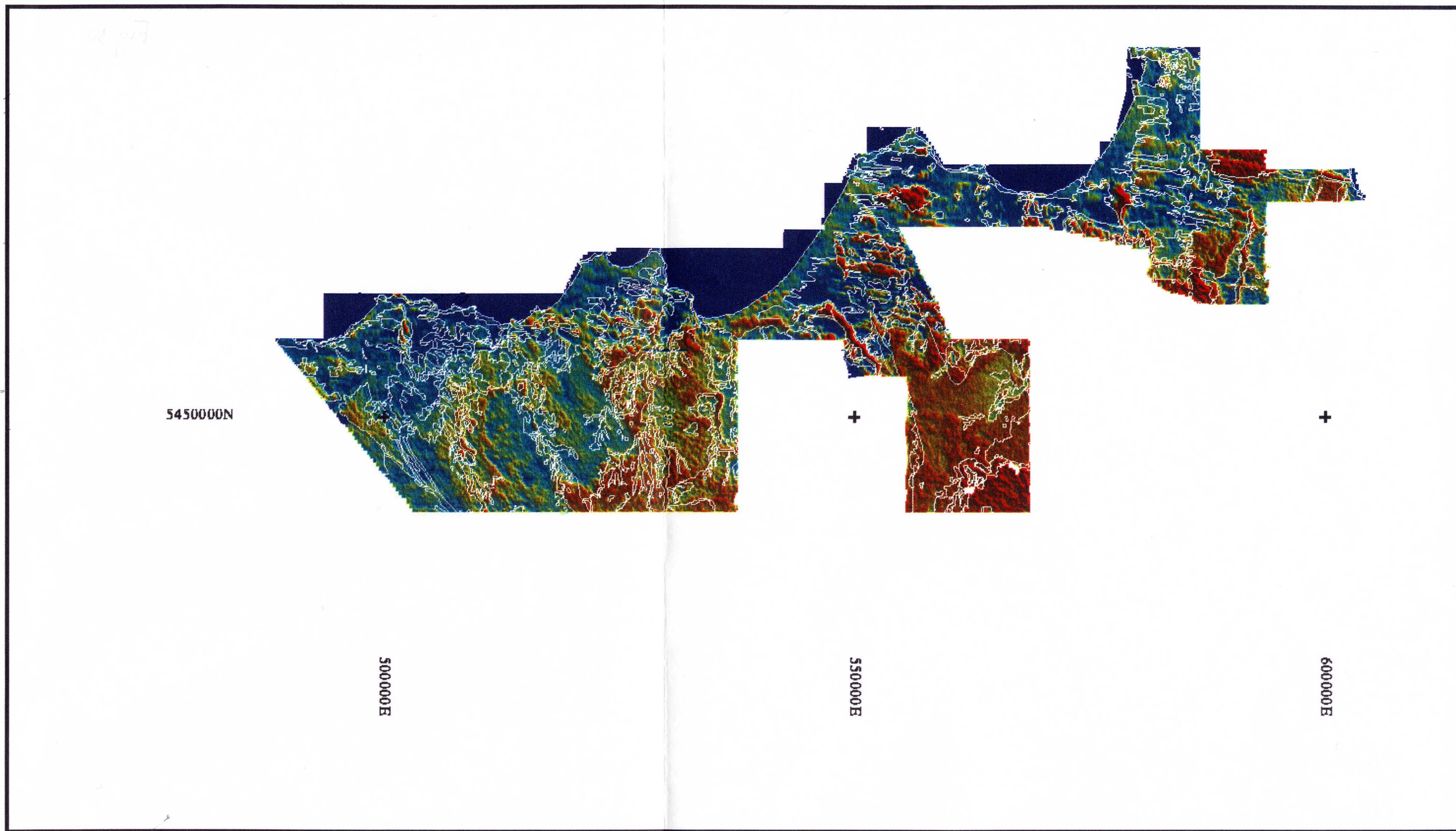


Figure 30

Radiometric total counts — NETGOLD northern coastal area.
 Polygons from the 1:250 000 digital geology shown in white.

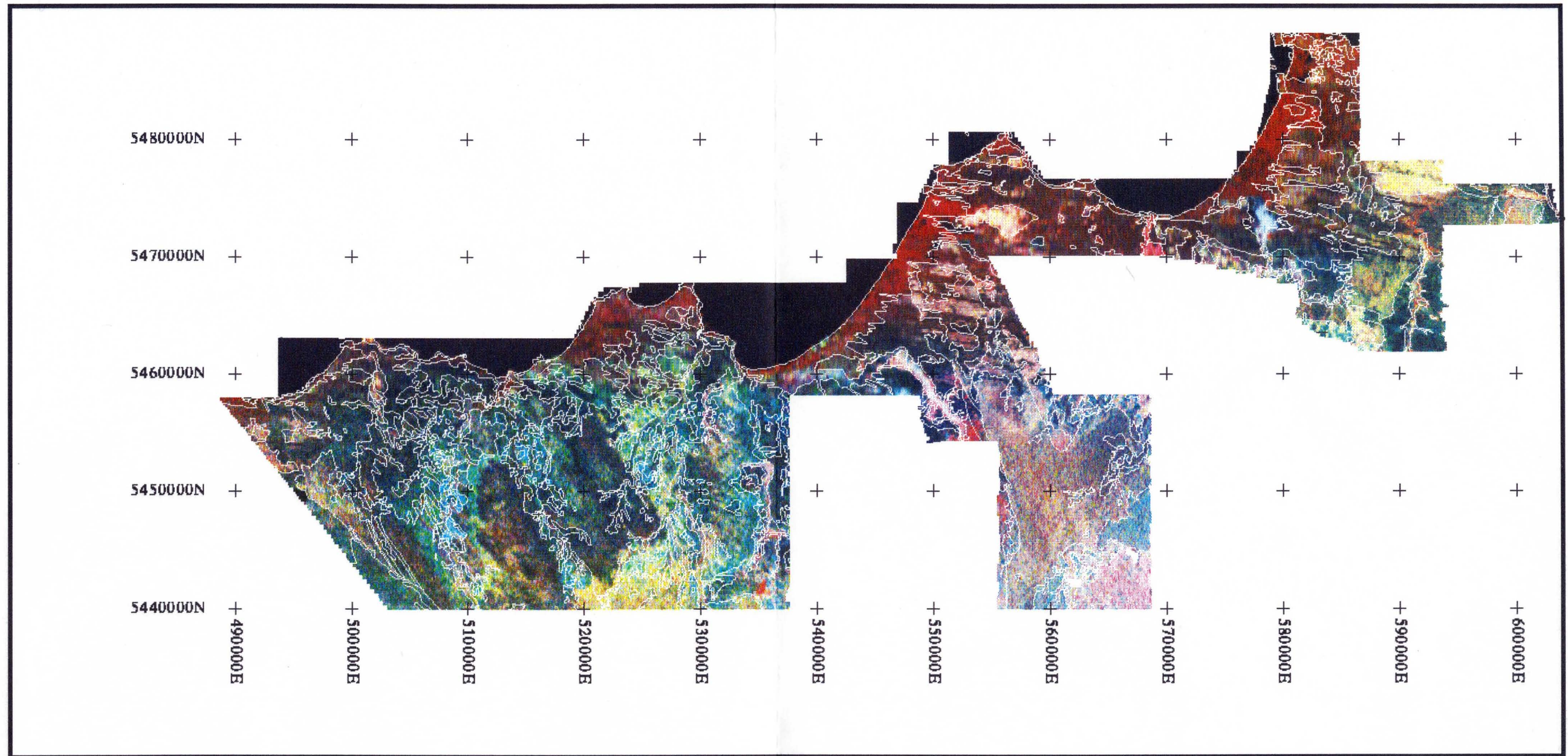
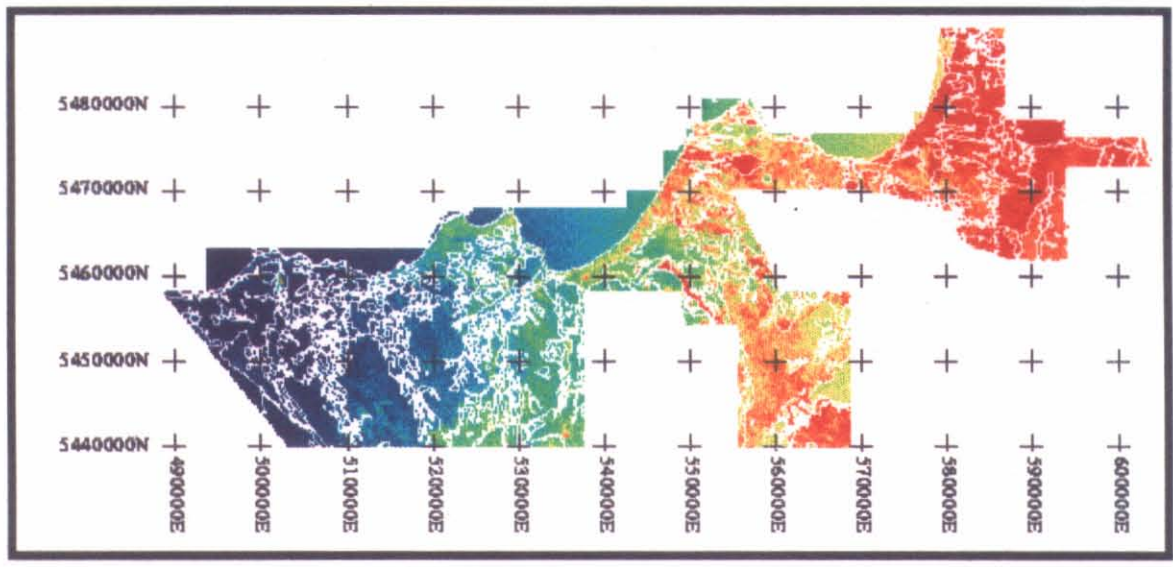
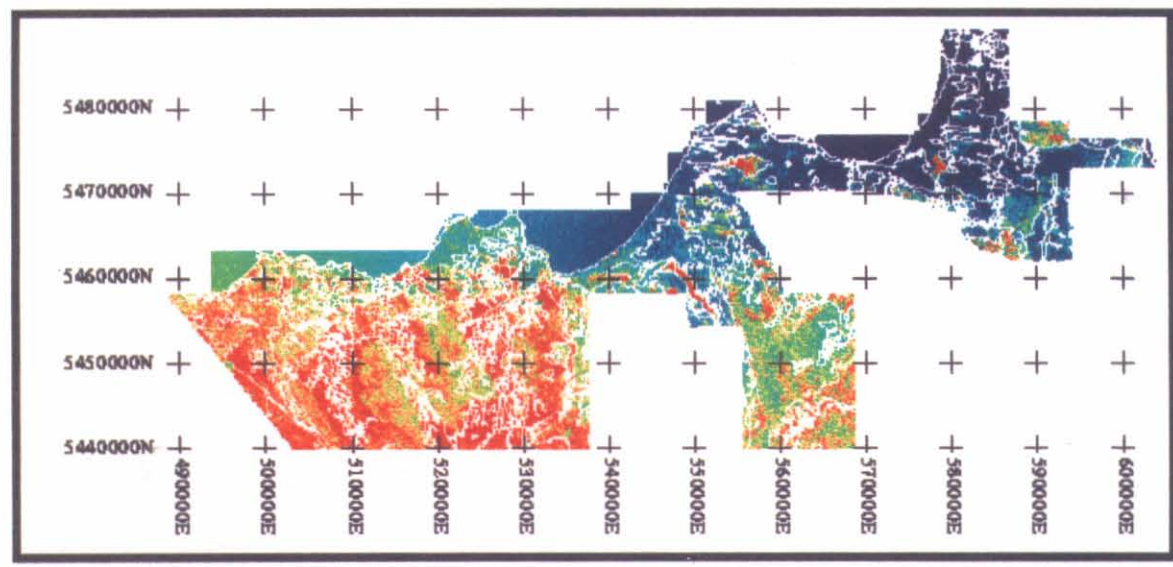


Figure 31

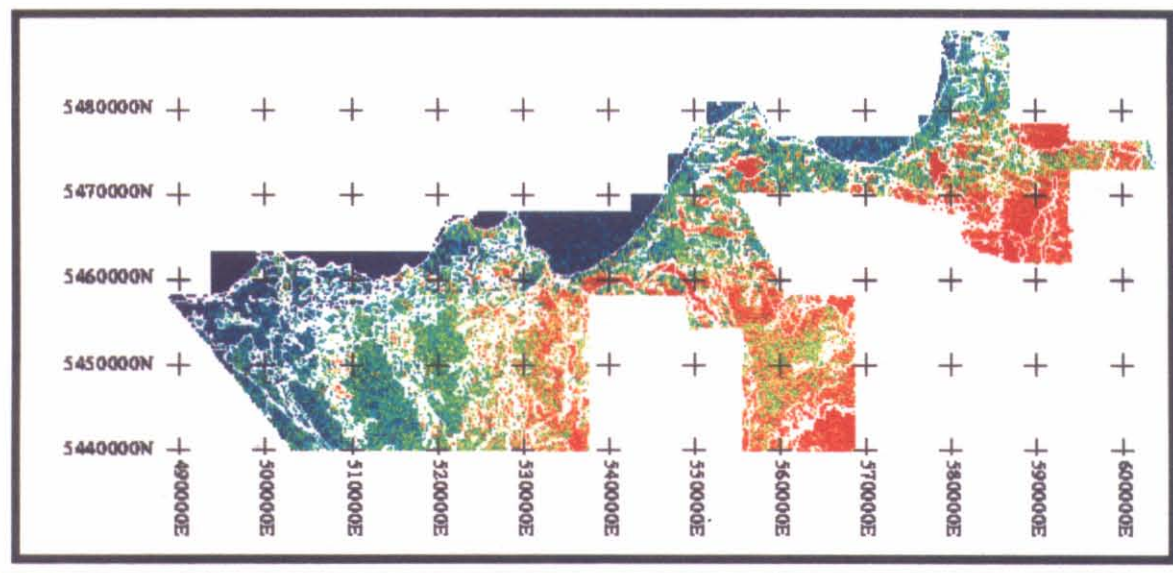
Radiometric element colour composite — NETGOLD northern coastal area.
 Polygons from the 1:250 000 digital geology shown in white (K=Red, Th=Green, U=Blue)



(a)
Potassium counts



(b)
Thorium counts



(c)
Uranium counts

Figure 32

Radiometric counts — NETGOLD northern coastal area.
Polygons from the 1:250 000 digital geology shown in white.